PDZK1 PDZ-1 and -4 Domains and NHERF1 PDZ-1 Domain Are Required for Interaction with OAT4-CT

PDZK1 possesses four PDZ domains and NHERF1 possesses two PDZ domains that assemble target proteins by binding to a CT that has a consensus PDZ motif (14). To check the possible interactions of the OAT4-CT with these PDZ domains of PDZK1 and NHERF1, we prepared prey vectors that contained the single PDZ domain of two PDZ proteins (PDZ-1, -2, -3, and -4 of PDZK1 and PDZ-1 and -2 of NHERF1). Interaction with OAT4-CT was observed when PDZ-1 and -4 were present but not with PDZ-2 and -3 of PDZK1 and when PDZ-1 was present but not with PDZ-2 of NHERF1 (Table 2).

In Vitro *Binding of OAT4 and PDZK1/NHERF1*

To confirm the ability of OAT4-CT to bind PDZK1 or NHERF1 *in vitro*, we next used the GST pulldown assay to validate the interaction (Figure 1). GST fusion proteins that bear the wild-type CT region of OAT4 (OAT4-CT-wt) or CT region mutants (OAT4-CT-d3) were used to pull down the full-length PDZK1 or the full-length NHERF1 proteins that were generated from *in vitro* translation experiments. The data demonstrated the same specificity of interaction for PDZK1/NHERF1 and OAT4 in the yeast two-hybrid assays. We did not observe the binding of PDZK1 and NHERF1 to OAT4-CT that lacked the PDZ motif (OAT4-CT-d3; Figure 1, A and B).

Co-Immunoprecipitation of OAT4 and PDZK1/NHERF1 from Heterologous Cells

To confirm further the interaction between OAT4 and PDZK1/NHERF1, we performed a co-immunoprecipitation study using the antibodies against human PDZK1 (19) and NHERF1(EBP50) in HEK293 cells. To test the specificity of EBP50 antibody, first we performed Western blot analysis of crude membranes from HEK293 cells that were transfected with vector (pcDNA3.1) alone (lane 1), with pcDNA3.1-hNHERF1 full length (lane 2), and with pcDNA3.1-hNHERF2 full length (Figure 1C, lane 3). A single strong band of approximately 50 kD, which is consistent with hNHERF1, was observed in lane 2 but not in lane 3. We coexpressed full-length human OAT4 fused with GFP (GFP-OAT4) and full-length PDZK1/NHERF1 in HEK293 cells. PDZK1 and NHERF1 were co-immunoprecipitated with a GFP-specific antibody in the lysates from the cells transfected with GFP-OAT4-wt, but neither PDZK1 nor NHERF1 was co-immunoprecipitated in those from the cells that were transfected with GFP-OAT4 that lacked the last three amino acids (Figure 1, D and E).

Comparison of Binding Affinities between OAT4-CT and Individual PDZ Domains of PDZK1 or NHERF1

To quantify and compare the interaction of OAT4 with PDZK1 and NHERF1, we performed surface plasmon resonance experiments using immobilized GST-OAT4-CT and mal-

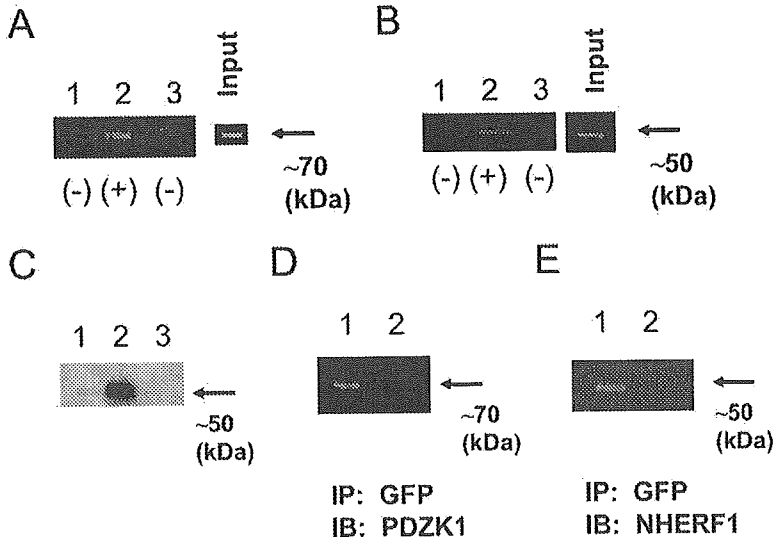

Figure 1. Interaction of PDZK1 and NHERF1 with organic anion transporter 4 (OAT4). (A and B) The *in vitro* translation products of full-length PDZK1 (A) or NHERF1 (B) using Transcend Biotinylated Lysine tRNA (Promega) were incubated with the GST alone (lane 1), GST-OAT4-CT-wt (lane 2), or GST-OAT4-CT-d3 (lane 3). The pulldown products were analyzed by SDS-PAGE. The input corresponds to the crude *in vitro* translation reaction. The positions of molecular mass standards are indicated on the right. (C) Western blot analysis of crude membranes from HEK293 cells that were transfected with vector (pcDNA3.1) alone (lane 1), with pcDNA3.1-hNHERF1 full length (lane 2), and with pcDNA3.1-hNHERF2 full length (lane 3). A single strong band of approximately 50 kD, which is consistent with NHERF1, was observed in lane 2 but not in lane 3. (D and E) Co-immunoprecipitation of the OAT4 and PDZK1 or NHERF1 proteins in HEK293 cells, respectively. HEK293 cells were transfected with pEGFP-C2 vectors encoding the wild-type full-length OAT4 (GFP-OAT4-FLwt, lane 1) or the full-length OAT4 that lacked the last three amino acid residues (GFP-OAT4-FLd3, lane 2) with pcDNA3.1-PDZK1 (D) or pcDNA3.1-NHERF1 (E) and then immunoprecipitated with anti-GFP antibody. Then, the immunoprecipitates were resolved by SDS-PAGE and probed with anti-PDZK1 antibodies (D) or with anti-EBP50 antibodies (E).

tose-binding protein (MBP)-fused PDZK1 PDZ domain 1, domain 4, and NHERF1 domain 1 proteins. As summarized in Table 3, the binding affinity for the PDZ domain 1 of PDZK1 showed high affinity (36 nM), that for the PDZ domain 4 of PDZK1 showed low affinity (1.2 μM), and that for the PDZ domain 1 of NHERF1 exhibited the lowest affinity (41.7 μM).

Tissue Distribution of OAT4 and PDZK1/NHERF1 mRNA in Human Tissues

In humans, OAT4 mRNA has been detected in both the kidney and the placenta (1); PDZK1 has been detected mainly in the liver, kidney, pancreas, gastrointestinal tract, and adrenal cortex (18); and NHERF1 has been detected ubiquitously (27). Using human multiple cDNA panels, we examined the mRNA distribution of OAT4, PDZK1, and NHERF1 to compare the tissue distribution and their overlaps. OAT4 transcripts were detected in the kidney, placenta, testis, small intestine, and colon, whereas PDZK1 and NHERF1 transcripts were detected in most of the tissues analyzed, confirming and expanding the previously described distribution in humans (Figure 2A). It is interesting that overlapping expressions among OAT4, PDZK1, and NHERF1 were limited to the kidney, placenta, and small intestine. This is the first time that OAT4 expression has been identified in the testis, small intestine, and colon.

Coexpression of OAT4, PDZK1, and NHERF1 in Human Kidney

OAT4 is present at the apical membrane of proximal tubules (2), and PDZK1 and NHERF1 have also been reported to be expressed in the same cells (19,27). To determine whether OAT4, PDZK1, and NHERF1 localize at the apical membrane of the renal proximal tubules, we performed immunostaining of human kidney sections with anti-OAT4, anti-PDZK1, and anti-NHERF1 antibodies. Consistent with previous reports, in the renal cortex, the overlapping expression of OAT4, PDZK1, and NHERF1 was detected at the apical membrane in most of the proximal tubular cells (Figure 2B).

OAT4 Transport Activities Are Increased in the Presence of PDZK1/NHERF1

To determine whether OAT4 and PDZK1/NHERF1 interactions are required to mediate the increase in OAT4 activity, we transfected HEK293 cells with the pcDNA3.1(+) construct that contained full-length OAT4 (OAT4-wt), OAT4 that lacked the last three amino acids (OAT4-d3), or OAT4 without insert (mock). At an incubation time of 2 min, we demonstrated that the uptake of [^{3}H]E_1S *via* both the OAT4-wt and OAT4-d3 was from five- to six-fold higher than that by the mock (Figure 3, A and B). E_1S transport activities in OAT4-wt were significantly increased after the coexpression of PDZK1 (1.4-fold; Figure 3A) as well as NHERF1 (1.2-fold; Figure 3B). These effects were abolished when OAT4-d3 was coexpressed with PDZK1 (Figure 3A) and NHERF1 (Figure 3B). These results indicate that the interaction between the OAT4-CT and PDZK1/NHERF1 is essential for the functional increase in OAT4-mediated E_1S transport.

Next, we examined the effect of the coexpression of two PDZ proteins on the kinetics of [^{3}H]E_1S transport *via* HEK293 cells that stably expressed OAT4 (HEK-OAT4) and that had been transfected with pcDNA3.1 vector alone, pcDNA3.1-PDZK1, or pcDNA3.1-NHERF1. Kinetic data showed that PDZK1 and NHERF1 significantly increased V_{max} from 86.5 to 123.6 and from 86.5 to 110.1 pmol/mg protein per min, respectively ($P < 0.05$), and did not change K_m (from 944 to 971 and from 944 to 1058, respectively), as compared with OAT4 transfected with vector alone (Figure 3C).

Surface Expression Level of OAT4 Protein

To determine changes in the cell surface expression level of OAT4, we used a cell membrane–impermeant biotinylation reagent to label cell-surface proteins selectively. After the treatment, cell lysates from HEK293 cells that stably expressed OAT4 that was transfected with hPDZK1, hNHERF1, or mock was collected. The amount of surface-biotinylated OAT4 expression on plasma membranes increased 1.3- to 1.4-fold (mock-transfected 30.0 ± 1.2, PDZK1-transfected 40.2 ± 2.6, NHERF1-transfected 42.5 ± 4.0 arbitrary units; $n = 3$) when PDZ proteins were coexpressed (Figure 4). These changes seem close to the one in V_{max} of OAT4-mediated transport observed in Figure 3C.

Discussion

Recent studies have shown that the PDZ domains function as modular protein–protein interaction motifs that serve to localize proteins to specific subcellular sites, to organize signaling cascades, and to regulate cell signaling (15–17). This domain binds to proteins that contain the tripeptide motif (S/T)-X-Ø

Table 3. Characteristics of interaction between OAT4 C-terminus and PDZK1 PDZ domain 1, domain 4, or NHERF1 PDZ domain 1[a]

Construct	k_a (1/mM per s)	k_d (1/min)	K_D (μM)
PDZK1-PDZ1	9.4×10^3	3.4×10^{-3}	0.036
PDZK1-PDZ4	6.8×10^2	7.9×10^{-4}	1.2
NHERF1-PDZ1	2.7×10^2	1.1×10^{-3}	42

[a]The kinetic characteristics of the interaction with immobilized GST-fused OAT4 C-terminus with the first and fourth PDZ domains of PDZK1 (PDZ1, 4) and the first PDZ domain of NHERF1 fused with maltose-binding protein measured by surface plasmon resonance methods are summarized. Association rate constants (k_a), dissociation rate constants (k_d), and equilibrium dissociation constants ($K_D = k_d/k_a$) are given.

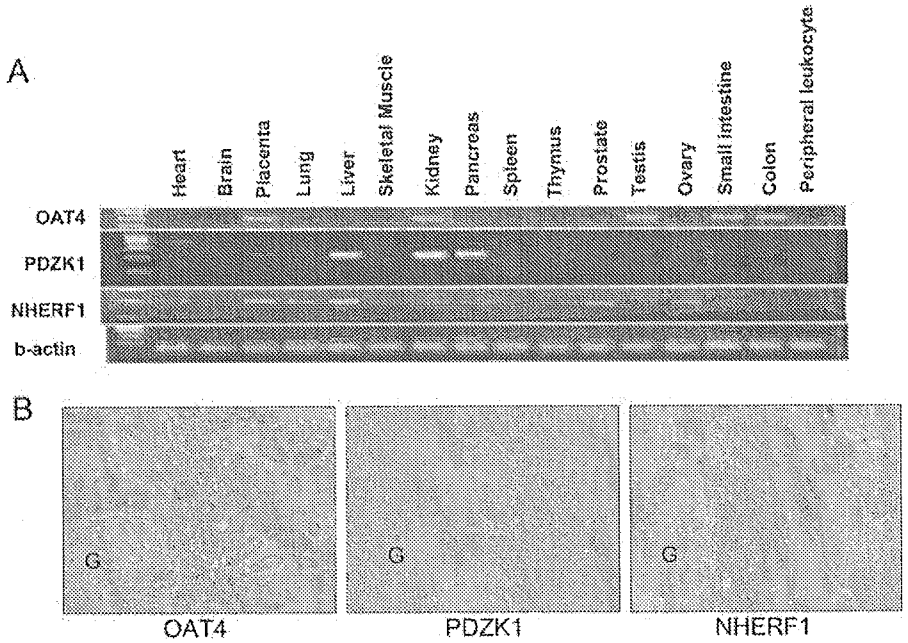

Figure 2. Localization of OAT4, PDZK1, and NHERF1. (A) Distribution of OAT4, PDZK1, and NHERF1 mRNA in human multiple cDNA panels. OAT4, PDZK1, and NHERF1 expression overlaps in the kidney, placenta, and small intestine. Control amplification with β-actin was performed in parallel (bottom). (B) Immunohistochemical analyses of OAT4, PDZK1, and NHERF1 in serial sections of human kidney. OAT4 was detected in the apical membrane of the proximal convoluted tubules (left), and no staining was observed in the basolateral membrane and glomeruli (G). PDZK1 (middle) and NHERF1 (right) were also detected in the apical membrane of the proximal convoluted tubules.

(X = any amino acid and Ø = a hydrophobic residue) at their CT (14). PDZ domains are also involved in receptor and ion channel clustering, to recruit kinases and phosphatases to their membrane-associated substrates. It has been postulated that the organic anion transporters, such as MRP2/4, NPT1, PEPT2, Oatp1, Oat-k1/k2, and CFEX (PAT1) that localize to the apical membrane and have the consensus PDZ-motif sequence at their CT, target the apical membrane mediated by PDZ proteins (28,29). Recently, we demonstrated that the urate/anion exchanger URAT1, one of the OAT family members, interacted with the PDZ protein PDZK1 *via* its CT (20). URAT1 was identified by *in silico* cloning using the sequence information of OAT4 (18). It is interesting that both clones have many similarities; for example, they show high sequence similarity (53%) and locate at the same gene locus, and their products localize at the apical membrane of the proximal tubules and are presumed to contribute the reabsorption of endogenous organic anions (urate and steroid sulfates) (5,18,20). Therefore, these similarities prompted us to examine the protein–protein interaction with well-known PDZ proteins such as PDZK1 and NHERF1 that are expressed at the apical side of the proximal tubules.

The E_1S transport study revealed that the coexpression of PDZK1 and/or NHERF1 with OAT4 in HEK293 cells leads to a significant enhancement of OAT4-mediated [^{3}H]E_1S transport. Kinetic studies of E_1S transport showed a significant increase (1.2- to 1.4-fold) in the V_{max} between PDZK1-, NHERF1-, and mock-transfected HEK293 cells (Figure 3C). In addition, the cell surface biotinylation experiment revealed that the augmentation of the E_1S transport activity was associated with the increased surface expression level of OAT4 protein from HEK-OAT4 cells and transfected with PDZK1 or NHERF1. These results are similar to those of the URAT1-PDZK1 interaction (20). Therefore, we speculated that both PDZK1 and NHERF1 have an equivalent potential for the stabilization and/or anchoring of OAT4 protein at the cell membrane, making it less likely to be internalized and subsequently degraded.

To date, some transporters that are localized at the apical membrane of epithelial cells, such as NaPi IIa, MRP2 (cMOAT), and CFTR, have been shown to bind with both PDZK1 and NHERF1 (24,29–34). As Gisler *et al.* (29) demonstrated, most of the mouse transporters that could bind with PDZK1 in the kidney also interacted with NHERF1. They also indicated that PDZK1 and NHERF1 could bind to each other. These results suggested that the scaffold under the plasma membrane is provided by the network of these PDZ proteins and forms an orchestrated assembly for membrane transport proteins (35,36). Among various couplings that are mediated by the PDZ proteins, the clustering of some organic anion transporters seems important for regulating the apical handling of organic anions (36). Although the binding affinities are >10-fold different (Table 3), both PDZK1 and NHERF1 demonstrated similar enhancement of OAT4-mediated E_1S transport activities. These results suggest the redundancy of the apical scaffolding network of the renal proximal tubules and might explain the absence of a significant phenotype in PDZK1 knockout mice (37). Double knockout of both NHERF1 and PDZK1 may reveal the significance of their overlapping specificities.

In the kidney, a large part of organic solutes is reabsorbed

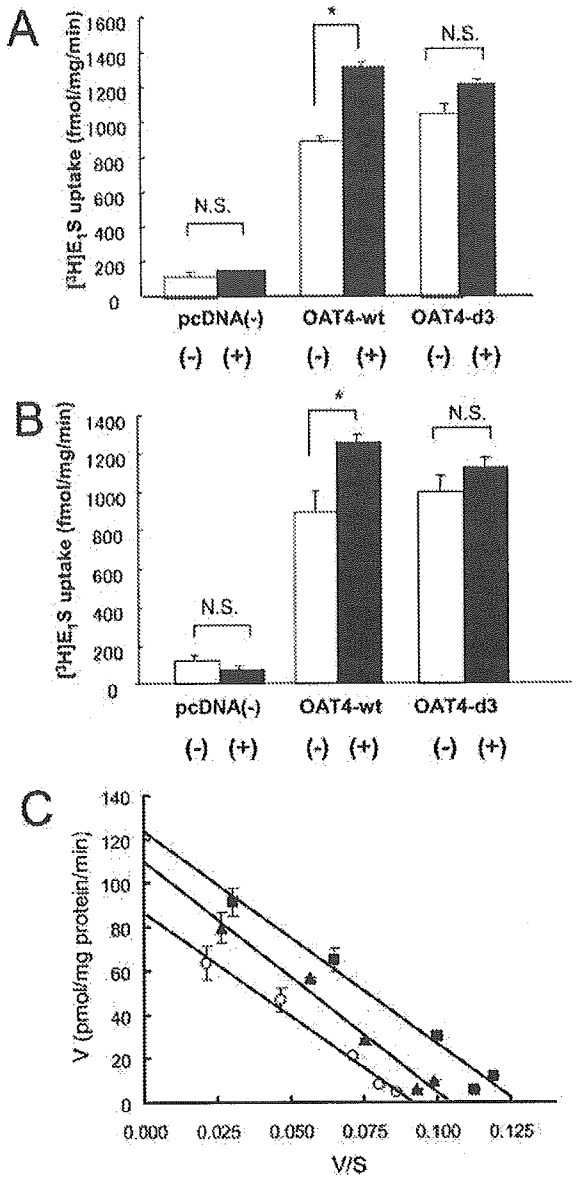

Figure 3. Effect of PDZK1 and NHERF1 on OAT4-mediated [^{3}H]estrone-3-sulfate (E_1S) transport activity. (A) Coexpression of OAT4 and PDZK1 increased E_1S uptake (50 nM) significantly compared with that by cells that were transfected with OAT4 alone. This effect was abolished when the C-terminal (CT) deletion mutant of OAT4 was co-transfected with PDZK1, confirming that the interaction of PDZK1 with the OAT4-CT domain is responsible for this effect. (B) Coexpression of OAT4 and NHERF1 increased E_1S uptake (50 nM) significantly compared with that by cells that were transfected with OAT4 alone. This effect was also abolished when the CT deletion mutant of OAT4 was co-transfected with NHERF1, confirming that the interaction of NHERF1 with the OAT4-CT domain is responsible for this effect. (C) Kinetic data using HEK293 cells that stably expressed OAT4 (HEK-OAT4) showed that PDZK1 (■) increased V_{max} from 86.5 to 123.6 pmol/mg protein per min and did not change K_m (from 944 to 971 μM), as compared with vector (pcDNA3.1) transfected (○). It also showed that NHERF1 (▲) increased the V_{max} from 86.5 to 110.1 pmol/mg protein per min and did not change K_m (from 944 to 1058 μM), compared with vector (pcDNA3.1) transfected (○). *$P < 0.05$.

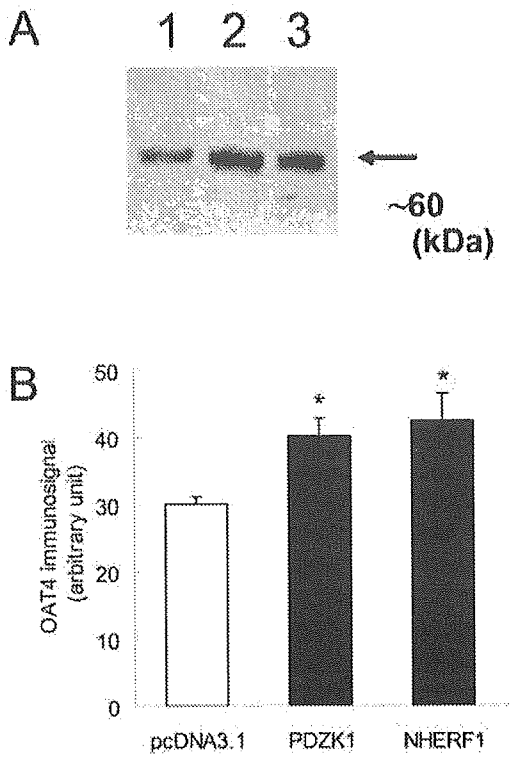

Figure 4. Surface expression level of OAT4. (A) cell surface biotinylation analysis of OAT4 that transiently expressed HEK293 cells that were transfected with pcDNA3.1 (vector alone; lane 1), those that were transfected with PDZK1 (lane 2), and those that were transfected with NHERF1 (lane 3). Single bands of approximately 60 kD, which are consistent with OAT4, were observed in both lanes. (B) Quantification of immunosignal for OAT4 ($n = 3$; bars are SD). *$P < 0.05$.

and secreted by specific transporters that are localized at the apical membrane of the proximal tubules. To achieve its concerted function, it seems plausible that transporters that exhibit similar functions couple functionally and physically. Following our recent report on URAT1 (20), here we found that OAT4 also sits on the scaffold of PDZK1 and NHERF1. In addition, the interaction between NPT1 CT and the third domain of PDZK1 was found in mouse (29) and in human (P.J., unpublished observations). NPT1 is an organic anion/Cl^- exchanger and may function as an exit pathway for some organic anions (11). Because neither OAT4 nor URAT1 bound with the third domain of PDZK1, the interaction between NPT1 CT and the third PDZ domain of PDZK1 enables us to speculate that the organic anion transport protein complex consisted of reabsorptive transporters (*e.g.*, OAT4, URAT1) and an efflux transporter (*e.g.*, NPT1) tethered by PDZ scaffolds (38). The close spatial positioning of functionally related transporter proteins may lead to the fast and efficient control of the transtubular transport for organic anions (39). Further study is necessary to address this issue.

Acknowledgments

This work was supported in part by grants from the Ministry of Education, Culture, Sports, Science and Technology of Japan; the Japan

Society for the Promotion of Science; Research on Health Sciences focusing on Drug Innovation from the Japan Health Sciences Foundation; Mutual Aid Corporation for Private Schools of Japan; the Tokyo Biochemical Research Foundation; the Nakatomi Foundation; the Salt Science Research Foundation (no. 0524); the Japan Foundation of Applied Enzymology; Heiwa Nakajima Foundation; and Health and Labor Sciences Research Grants for Research on Advanced Medical Technology: Toxicogenomics Project.

Part of this work was presented at the 36th Annual Meeting and Scientific Exposition of the American Society of Nephrology, San Diego, CA, October 2003.

We thank Akie Toki and Keiko Sakama for technical assistance. The anti-PDZK1 and anti-OAT4 polyclonal antibodies were supplied by Transgenic Inc. (Kumamoto, Japan).

References

1. Cha SH, Sekine T, Kusuhara H, Yu E, Kim JY, Kim DK, Sugiyama Y, Kanai Y, Endou H: Molecular cloning and characterization of multispecific organic anion transporter 4 expressed in the placenta. *J Biol Chem* 275: 4507–4512, 2000
2. Babu E, Takeda M, Narikawa S, Kobayashi Y, Enomoto A, Tojo A, Cha SH, Sekine T, Sakthisekaran D, Endou H: Role of human organic anion transporter 4 in the transport of ochratoxin A. *Biochim Biophys Acta* 1590: 64–75, 2002
3. Miyazaki H, Sekine T, Endou H: The multispecific organic anion transporter family: Properties and pharmacological significance. *Trends Pharmacol Sci* 25: 654–662, 2004
4. Ugele B, St-Pierre MV, Pihusch M, Bahn A, Hantschmann P: Characterization and identification of steroid sulfate transporters of human placenta. *Am J Physiol Endocrinol Metab* 284: E390–E398, 2003
5. Ekaratanawong S, Anzai N, Jutabha P, Miyazaki H, Noshiro R, Takeda M, Kanai Y, Sophasan S, Endou H: Human organic anion transporter 4 is a renal apical organic anion/dicarboxylate exchanger in the proximal tubules. *J Pharmacol Sci* 94: 297–304, 2004
6. Pajor AM: Molecular properties of sodium/dicarboxylate cotransporters. *J Membr Biol* 175: 1–8, 2000
7. Dantzler WH: Renal organic anion transport: A comparative and cellular perspective. *Biochim Biophys Acta* 1566: 169–181, 2002
8. Leier I, Hummel-Eisenbeiss J, Chi Y, Keppler D: ATP-dependent para-aminohippurate transport by apical multidrug resistance protein MRP2. *Kidney Int* 57: 1636–1642, 2000
9. van Aubel RAMH, Peters JGP, Masereeuw R, van Os CH, Russel FGM: Multidrug resistance protein Mrp2 mediates ATP-dependent transport of classic renal organic anion p-aminohippurate. *Am J Physiol Renal Physiol* 279: F713–F717, 2000
10. van Aubel RA, Smeets PH, Peters JG, Bindels RJ, Russel FG: The MRP4/ABCC4 gene encodes a novel apical organic anion transporter in human kidney proximal tubules: Putative efflux pump for urinary cAMP and cGMP. *J Am Soc Nephrol* 13: 595–603, 2002
11. Smeets PH, van Aubel RA, Wouterse AC, van den Heuvel JJ, Russel FG: Contribution of multidrug resistance protein 2 (MRP2/ABCC2) to the renal excretion of p-aminohippurate (PAH) and identification of MRP4 (ABCC4) as a novel PAH transporter. *J Am Soc Nephrol* 15: 2828–2835, 2004
12. Uchino H, Tamai I, Yamashita K, Minemoto Y, Sai Y, Yabuuchi H, Miyamoto K, Takeda E, Tsuji A: p-Aminohippuric acid transport at renal apical membrane mediated by human inorganic phosphate transporter NPT1. *Biochem Biophys Res Commun* 270: 254–259, 2000
13. Jutabha P, Kanai Y, Hosoyamada M, Chairoungdua A, Kim DK, Iribe Y, Babu E, Kim JY, Anzai N, Chatsudthipong V, Endou H: Identification of a novel voltage-driven organic anion transporter present at apical membrane of renal proximal tubule. *J Biol Chem* 278: 27930–27938, 2003
14. Songyang Z, Fanning AS, Fu C, Xu J, Marfatia SM, Chishti AH, Crompton A, Chan AC, Anderson JM, Cantley LC: Recognition of unique carboxyl-terminal motifs by distinct PDZ domains. *Science* 275: 73–77, 1997
15. Fanning AS, Anderson JM: Protein modules as organizers of membrane structure. *Curr Opin Cell Biol* 11: 432–439, 1999
16. Garner CC, Nash J, Huganir RL: PDZ domains in synapse assembly and signalling. *Trends Cell Biol* 10: 274–280, 2000
17. Hung AY, Sheng M: PDZ domains: Structural modules for protein complex assembly. *J Biol Chem* 277: 5699–5702, 2002
18. Enomoto A, Kimura H, Chairoungdua A, Shigeta Y, Jutabha P, Cha SH, Hosoyamada M, Takeda M, Sekine T, Igarashi T, Matsuo H, Kikuchi Y, Oda T, Ichida K, Hosoya T, Shimokata K, Niwa T, Kanai Y, Endou H: Molecular identification of a renal urate-anion exchanger that regulates blood urate levels. *Nature* 417: 447–452, 2002
19. Kocher O, Comella N, Tognazzi K, Brown LF: Identification and partial characterization of PDZK1: A novel protein containing PDZ interaction domains. *Lab Invest* 78: 117–125, 1998
20. Anzai N, Miyazaki H, Noshiro R, Khamdang S, Chairoungdua A, Enomoto A, Hirata T, Shin HJ, Sakamoto S, Tomita K, Kanai Y, Endou H: The multivalent PDZ domain-containing protein PDZK1 regulates transport activity of renal urate-anion exchanger URAT1 via its C-terminal. *J Biol Chem* 279: 45942–45950, 2004
21. Anzai N, Deval E, Schaefer L, Friend V, Lazdunski M, Lingueglia E: The multivalent PDZ domain-containing protein CIPP is a partner of acid-sensing ion channel 3 in sensory neurons. *J Biol Chem* 277: 16655–16661, 2002
22. Malmqvist M: Biospecific interaction analysis using biosensor technology. *Nature* 361: 186–187, 1993
23. Rochdi MD, Watier V, La Madeleine C, Nakata H, Kozasa T, Parent JL: Regulation of GTP-binding protein alpha q (Galpha q) signaling by the ezrin-radixin-moesin-binding phosphoprotein-50 (EBP50). *J Biol Chem* 277: 40751–40759, 2002
24. Shenolikar S, Weinman EJ: NHERF: Targeting and trafficking membrane proteins. *Am J Physiol Renal Physiol* 280: F389–F395, 2001
25. Scott RO, Thelin WR, Milgram SL: A novel PDZ protein regulates the activity of guanylyl cyclase C, the heat-stable enterotoxin receptor. *J Biol Chem* 277: 22934–22941, 2002
26. Wade JB, Liu J, Coleman RA, Cunningham R, Steplock DA, Lee-Kwon W, Pallone TL, Shenolikar S, Weinman EJ: Localization and interaction of NHERF isoforms in the renal proximal tubule of the mouse. *Am J Physiol Cell Physiol* 285: C1494–C1503, 2003
27. Yun CHC, Oh S, Zizak M, Steplock D, Tsao S, Tse C-M, Weinman EJ, Donowitz M: cAMP-mediated inhibition of the epithelial brush border Na+/H+ exchanger, NHE3,

requires an associated regulatory protein. *Proc Natl Acad Sci U S A* 94: 3010–3015, 1997
28. Russel FGM, Masereeuw R, van Aubel RAMH: Molecular aspects of renal anionic drug transport. *Annu Rev Physiol* 64: 563–594, 2002
29. Gisler SM, Pribanic S, Bacic D, Forrer P, Gantenbein A, Sabourin LA, Tsuji A, Zhao ZS, Manser E, Biber J, Murer H: PDZK1: I. A major scaffolder in brush borders of proximal tubular cells. *Kidney Int* 64: 1733–1745, 2003
30. Gisler SM, Stagljar I, Traebert M, Bacic D, Biber J, Murer H: Interaction of the type IIa Na/Pi cotransporter with PDZ proteins. *J Biol Chem* 276: 9206–9213, 2001
31. Wang S, Yue H, Derin RB, Guggino WB, Li M: Accessory protein facilitated CFTR-CFTR interaction, a molecular mechanism to potentiate the chloride channel activity. *Cell* 103: 169–179, 2000
32. Kocher O, Comella N, Gilchrist A, Pal R, Tognazzi K, Brown LF, Knoll JHM: PDZK1, a novel PDZ domain-containing protein up-regulated in carcinomas and mapped to chromosome 1q21, interacts with cMOAT (MRP2), the multidrug resistance-associated protein. *Lab Invest* 79: 1161–1170, 1999
33. Raghuram V, Mak DD, Foskett JK: Regulation of cystic fibrosis transmembrane conductance regulator single-channel gating by bivalent PDZ-domain-mediated interaction. *Proc Natl Acad Sci U S A* 98: 1300–1305, 2001
34. Hegedus T, Sessler T, Scott R, Thelin W, Bakos E, Varadi A, Szabo K, Homolya L, Milgram SL, Sarkadi B: C-terminal phosphorylation of MRP2 modulates its interaction with PDZ proteins. *Biochem Biophys Res Commun* 302: 454–461, 2003
35. Biber J: Emerging roles of transporter-PDZ complexes in renal proximal tubular reabsorption. *Pflugers Arch* 443: 3–5, 2001
36. Moe OW: Scaffolds: Orchestrating proteins to achieve concerted function. *Kidney Int* 64: 1916–1917, 2003
37. Kocher O, Pal R, Roberts M, Cirovic C, Gilchrist A: Targeted disruption of the PDZK1 gene by homologous recombination. *Mol Cell Biol* 23: 1175–1180, 2003
38. Anzai N, Jutabha P, Kanai Y, Endou H: Integrated physiology of proximal tubular organic anion transport. *Curr Opin Nephrol Hypertens* 14: 472–479, 2005
39. Brone B, Eggermont J: PDZ proteins retain and regulate membrane transporters in polarized epithelial cell membranes. *Am J Physiol Cell Physiol* 288: C20–C29, 2005

0022-3565/05/3152-534–544$20.00
THE JOURNAL OF PHARMACOLOGY AND EXPERIMENTAL THERAPEUTICS

JPET 315:534–544, 2005

Vol. 315, No. 2
88583/3057263
Printed in U.S.A.

Functional Characterization of Rat Organic Anion Transporter 5 (*Slc22a19*) at the Apical Membrane of Renal Proximal Tubules

Naohiko Anzai, Promsuk Jutabha, Atsushi Enomoto, Hirokazu Yokoyama, Hiroshi Nonoguchi, Taku Hirata, Katsuko Shiraya, Xin He, Seok Ho Cha, Michio Takeda, Hiroki Miyazaki, Takeshi Sakata, Kimio Tomita, Takashi Igarashi, Yoshikatsu Kanai, and Hitoshi Endou

Department of Pharmacology and Toxicology, Kyorin University School of Medicine, Mitaka-shi, Tokyo, Japan (N.A., P.J., A.E., H.Y., T.H., K.S., X.H., S.H.C., M.T., H.M., T.S., Y.K., H.E.); Department of Pediatrics, Graduate School of Medicine, University of Tokyo, Bunkyo-ku, Tokyo, Japan (H.Y., T.I.); and Department of Nephrology, Graduate School of Medical Sciences, Kumamoto University, Kumamoto-shi, Kumamoto, Japan (H.N., H.M., K.T.)

Received April 25, 2005; accepted August 1, 2005

ABSTRACT

A novel member of the organic anion transporter (OAT) family, Oat5 (*Slc22a19*), has been reported to transport a naturally occurring mycotoxin, ochratoxin A (OTA). However, neither its endogenous substrate and driving force nor physiological functions have been determined. Herein, we report the functional characterization of rat Oat5 (rOat5), as well as its intrarenal distribution and membrane localization. When expressed in *Xenopus laevis* oocytes, rOat5 mediated the transport of sulfate conjugates of steroids such as estrone-3-sulfate (E_1S; K_m = 18.9 ± 3.9 μM) and dehydroepiandrosterone sulfate (K_m = 2.3 ± 0.2 μM) in a sodium-independent manner, in addition to OTA. The rOat5-mediated E_1S transport was strongly inhibited by four-carbon (C4) dicarboxylate succinate and longer dicarboxylates (C7–C9). The uptake of [^{3}H]E_1S via rOat5 was significantly *trans*-stimulated by succinate, and the efflux of [^{14}C]succinate was significantly *trans*-stimulated by E_1S. A similar *trans*-stimulatory effect of preloaded succinate on E_1S uptake was also detected in cells stably expressing rOat5 (S_2 rOat5). rOat5 interacted with chemically heterogenous anionic compounds. The rOat5-mediated E_1S transport was inhibited by several sulfate conjugates, such as 4-methylumbelliferyl sulfate and β-estradiol sulfate, but not by glucuronide conjugates. An immunohistochemical study showed that rOat5 was localized at the apical membrane of renal proximal tubules in the corticomedullary region. rOat5 mRNA was expressed in the late segments (S_2 and S_3) of proximal tubules. These results indicate that rOat5 is renal organic anion/dicarboxylates exchanger and, under physiological conditions, may function as an apical reabsorptive pathway for organic anions in proximal tubules driven by an outward gradient of dicarboxylates.

This work was supported in part by grants from the Japanese Ministry of Education, Culture, Sports, Science and Technology (grants-in-aid for Scientific Research and High-Tech Research Center), the Science Research Promotion Fund of the Japan Private School Promotion Foundation, Research on Health Sciences Focusing on Drug Innovation from the Japan Health Sciences Foundation, grants-in-aid for Scientific Research from the Japan Society for the Promotion of Science (JSPS), grants-in-aid from the Salt Science Research Foundation (no. 0524), and Health and Labor Sciences Research Grants for Research on Advanced Medical Technology: Toxicogenomics Project. P.J. is a research fellow supported by the Labor Sciences Research Grants for Research on Advanced Medical Technology: Toxicogenomics Project.

Part of this work was presented at the 36th Annual Meeting and Scientific Exposition of the American Society of Nephrology, San Diego, CA, October 2003.

N.A. and P.J. contributed equally to this work.

Article, publication date, and citation information can be found at http://jpet.aspetjournals.org.

doi:10.1124/jpet.105.088583.

The kidney plays an important role in the elimination of harmful endogenous compounds and xenobiotics from the body. The proximal tubule is the primary site where numerous organic anions are taken up from the blood and excreted into the urine (Wright and Dantzler, 2004). The transcellular secretion of organic anions in the proximal tubule involves a two-step process: 1) the uptake of organic anions across the basolateral membrane of proximal tubular cells and 2) their excretion across the apical membrane into the tubular lumen. The former is energetically uphill and is accomplished by a tertiary active process via the organic anion/dicarboxylate exchanger that uses the outwardly directed gradient of

ABBREVIATIONS: OAT/Oat, organic anion transporter; PAH, *para*-aminohippuric acid; rOat5, rat Oat5; BBMV, brush-border membrane vesicle; NPT/Npt, sodium-dependent inorganic phosphate transporter; MRP/Mrp, multidrug resistance-associated protein; OATP/oatp, organic anion-transporting polypeptide(s); MAL, medullarly thick ascending limb; OAT_V1, voltage-driven organic anion transporter; EST, expressed sequence tag; E_1S, estrone-3-sulfate; DHEAS, dehydroepiandrosterone sulfate; OTA, ochratoxin A; NaDC, Na^+-dependent dicarboxylate transporter; HEK, human embryonic kidney; PCR, polymerase chain reaction; S_1, S_2, S_3, the first, second, and third segments of proximal tubule, respectively; hOAT, human OAT; D-PBS, Dulbecco's modified phosphate-buffered saline; RT, reverse transcription; CCD, cortical collecting duct.

five-carbon (C5) dicarboxylate α-ketoglutarate, one of the Krebs-cycle intermediates (Burckhardt et al., 2001). Two organic anion transporter (OAT) proteins, OAT1 (Sekine et al., 1997; Sweet et al., 1997; Wolff et al., 1997) and OAT3 (Kusuhara et al., 1999; Bakhiya et al., 2003; Sweet et al., 2003), have been proposed to be responsible for this step. The latter process is believed to be transporter-mediated, although this process is energetically downhill. In general, the efflux system for *para*-aminohippurate (PAH; a prototypical substrate for the organic anion transport system) in the brush-border (apical) membrane has been investigated using brush-border membrane vesicles (BBMVs). The electroneutral anion exchange systems and voltage-driven transport systems are considered to play a physiological role not only in the efflux of various organic anions but also in the reabsorption of some organic anions. However, the precise mechanism underlying the apical organic anion transport still remains unclear.

To date, several cDNAs encoding renal organic anion transporters have been successively identified in the kidney, including OAT, organic anion-transporting polypeptide (oatp), sodium-dependent inorganic phosphate transporter (NPT), and multidrug resistance-associated protein (MRP) families (Burckhardt et al., 2001; Russel et al., 2002). OAT4 (human), Oatp1 (rodent), Oat-k1/k2 (rodents), and NPT1 (human and mouse) are localized at the apical membrane of proximal tubules and are the possible candidates for an anion-exchange system. Regarding the ATP-driven organic anion transport system, MRP2 and MRP4 are also localized at the apical membrane of proximal tubules, although the relative contributions of both transporters to the apical efflux of organic anions have yet to be identified (Russel et al., 2002; van Aubel et al., 2002; Smeets et al., 2004). Recently, we have identified a novel voltage-driven organic anion transporter (OAT_V1) at the apical membrane of pig renal proximal tubules (Jutabha et al., 2003). OAT_V1 seems to be the long-hypothesized potential-driven facilitator in pig BBMVs (Werner et al., 1990; Krick et al., 2000). OAT_V1 exhibits the highest amino acid sequence identity to NPT1 (60–65%), although the functional properties of both transporters are different. Therefore, it should be elucidated whether OAT_V1 is an ortholog of human NPT1 (Uchino et al., 2000). NPT1 was suggested to be a good candidate for the apical potential-driven facilitator in human proximal tubules characterized in earlier experiments on BBMVs.

The number of OAT isoforms is rapidly increasing to date. Among them, both human and rodent cDNAs for OAT1 to OAT3 were reported, whereas only human cDNA was cloned for OAT4 (Koepsell and Endou, 2004). Very recently, Youngblood and Sweet (2004) reported the novel murine organic anion transporter mOat5 (*Slc22a19*) expressed in the kidney. They demonstrated that mOat5 mediates the transport of mycotoxin ochratoxin A (OTA), but their study was very limited. For example, they could not determine its endogenous substrate and driving force or its intrarenal localization related to its physiological functions. In the present study, we isolated this novel OAT member Oat5 from the rat kidney by a homology search of an expressed sequence tag (EST) database using a human OAT4 sequence. Rat Oat5 (rOat5) mediates the sodium-independent transport of sulfate conjugates of steroids, such as estrone-3-sulfate (E_1S) and dehydroepiandrosterone sulfate (DHEAS) as well as OTA. The most surprising finding of our study was that rOat5 interacted with succinate, which has not been reported as a counterion for the classical renal organic anion transport system to date, to mediate organic anion/succinate exchange. These data indicate that rOat5 is renal organic anion transporter that may mainly function as an apical pathway for the reabsorption of some organic anions driven by an outward gradient of dicarboxylates, including succinate. The functional characterization of rOat5 deepens our understanding of renal apical transport mechanisms of organic anions, including xenobiotics and endogenous compounds.

Materials and Methods

Materials. [^{3}H]E_1S (2.0 TBq/mmol) and [^{3}H]DHEAS (520 GBq/mmol) were purchased from PerkinElmer Life and Analytical Sciences (Boston, MA). [^{3}H]Ochratoxin A (OTA) (547.6 GBq/mmol) was purchased from Moravek Biochemicals (Brea, CA). [^{14}C]Succinate (4.07 GBq/mmol) was from American Radiolabeled Chemicals, Inc. (St. Louis, MO). [^{32}P]dCTP was obtained from GE Healthcare (Little Chalfont, Buckinghamshire, UK). All other chemicals and reagents were of analytical grade and obtained from commercial sources.

Isolation of rOat5 cDNA. The EST database was searched for "query human OAT4 (hOAT4)", and an EST clone (GenBank accession number AI058341) was identified. The [^{32}P]dCTP-labeled probe was synthesized from this clone (I.M.A.G.E. ID No. UI-*R*-C1-kn-d-03-0-UI) and used for the screening of a rat kidney cDNA library. A nondirectional cDNA library was prepared from rat kidney poly(A)$^+$ RNA using the Superscript Choice System (Invitrogen, Carlsbad, CA). The cDNA library was screened as described previously (Kusuhara et al., 1999). rOat5 cDNA was sequenced in both directions by the dye terminator cycle-sequencing method using an ABI PRISM 3100 genetic analyzer (Applied Biosystems, Foster City, CA).

Functional Characterization in *Xenopus laevis* Oocytes. cRNA synthesis and radiolabeled substrate uptake measurements were performed as described elsewhere (Kusuhara et al., 1999). Capped cRNA was synthesized in vitro using SP6 RNA polymerase from plasmid DNA linearized with RsrII. Defolliculated stage IV and stage V oocytes were injected with 25 ng of capped rOat5 cRNA and incubated in modified Barth's solution [88 mM NaCl, 1 mM KCl, 0.33 mM $Ca(NO_3)_2$, 0.4 mM $CaCl_2$, 0.8 mM $MgSO_4$, 2.4 mM $NaHCO_3$, and 10 mM HEPES] containing 50 μg/ml gentamicin at 18°C. After two to three days of incubation, uptake and efflux experiments were performed at room temperature using ND96 solution (96 mM NaCl, 2 mM KCl, 1.8 mM $CaCl_2$, 1 mM $MgCl_2$, and 5 mM HEPES, pH 7.4).

Kinetic parameters for the uptake of E_1S, DHEAS, and OTA via rOat5 were estimated from the following equation: $v = V_{max} \times S/(K_m + S)$, where v is the rate of substrate uptake (picomole/oocyte/hour), S is the substrate concentration in the medium (in micromolars), K_m is the Michaelis-Menten constant (in micromolars), and V_{max} is the maximum uptake rate (picomole/oocyte/hour). These kinetic parameters were determined with the Eadie-Hofstee equation.

To examine the *trans*-stimulatory effect of both the uptake and efflux of radiolabeled substrates, 50 nl of [^{14}C]succinate (~2 mM) or cold succinate (50 mM) was injected into oocytes expressing rOat5 with a fine-tipped glass micropipette as described previously (Jutabha et al., 2003). Individual oocytes then were washed with ice-cold ND96 solution twice, placed on ice for 5 min, incubated with ND96 at room temperature for 1 h, and then finally transferred into a medium with or without radiolabeled E_1S or unlabeled E_1S and incubated at room temperature for 1 h. Radioactivity in both the medium and oocytes was determined after a 1-h incubation.

For the uptake and efflux measurements in the present study, 8 to 10 oocytes were used for each data point. The values are expressed as mean ± S.E. We repeated each experiment at least twice to confirm the results. The results from representative experiments are shown in the figures.

Cell Culture and Establishment of S_2 rOat5. The establishment of cells stably expressing rOat5 (S_2 rOat5) was carried out as described previously (Takeda et al., 2002). These cells were grown in a humidified incubator at 33°C and under 5% CO_2 using the RITC 80-7 medium containing 5% fetal bovine serum, 10 μg/ml transferrin, 0.08 U/ml insulin, 10 ng/ml recombinant epidermal growth factor, and 400 μg/ml geneticin. The cells were subcultured in a medium containing 0.05% trypsin-EDTA solution (containing 137 mM NaCl, 5.4 mM KCl, 5.5 mM glucose, 4 mM $NaHCO_3$, 0.5 mM EDTA, and 5 mM HEPES, pH 7.2) and subjected to 25 to 35 passages.

Uptake Study Using S_2 rOat5. Uptake experiments were performed as described previously (Takeda et al., 2002). Organic anion transport in S_2 rOat5 was estimated by measuring the uptake rates of [^{3}H]E_1S and [^{14}C]succinate. S_2 rOat5 or S_2 pcDNA 3.1(+) (S_2 mock) cells (1×10^5 cells) were plated on 24-well plates and cultured for two days. After the medium was removed, cell monolayers were washed twice with Dulbecco's modified phosphate-buffered saline (D-PBS) (containing 137 mM NaCl, 3 mM KCl, 8 mM Na_2HPO_4, 1 mM KH_2PO_4, 1 mM $CaCl_2$, and 0.5 mM $MgCl_2$, pH 7.4) supplemented with 5.5 mM D-glucose, and preincubated for 10 min. The monolayers then were incubated with 500 μl of D-PBS containing 50 nM [^{3}H]E_1S or 10 μM [^{14}C]succinate for 2 min at 37°C. The cells were washed three times with ice-cold D-PBS and solubilized in 0.5 ml of 0.1 N sodium hydroxide. The amount of substrate accumulated within the cells was then determined by measuring radioactivity.

To clarify the driving force and its transport direction, we examined the *trans*-stimulatory effect of succinate on rOat5-mediated E_1S transport as described elsewhere (Ekaratanawong et al., 2004). For the experiments on the uptake of radiolabeled substrates, the cells were prepared as described above. In particular, the cells were preloaded with 0.5 ml of D-PBS with or without unlabeled substrates (5 mM succinate or glutarate) at 37°C for 30 min before uptake experiments.

Preparation of Anti-rOat5 Antibody. We generated a rabbit anti-rOat5 polyclonal antibody raised against a keyhole limpet hemocyanin-conjugated synthesized peptide REVKKDAVAKVTPF (538–551 of the amino acid sequence) corresponding to the 14 amino acids of the COOH terminus of rOat5.

Transfection, Crude Membrane Preparation, and Western Blot. Cell culture and transfection of HEK293 cells and the preparation of its crude membrane fractions were carried out as described previously (Anzai et al., 2004). pcDNA3.1-rOat5 or pcDNA3.1 vector (2 μg) was transfected into HEK293 cells.

Immunohistochemical Analysis. After anesthetizing the rats, their kidneys were perfused in situ with 4% paraformaldehyde-phosphate-buffered saline and excised. Kidney slices (2–3-mm thick) were fixed in the same solution at room temperature overnight and embedded in paraffin. Two-micrometer-thick sections were prepared, and after deparaffinization, the sections were incubated in 3% H_2O_2 for 15 min to abrogate endogenous peroxidase activity. Blocking was performed with 10% goat serum for 20 min. Then, the sections were further incubated overnight at 4°C with the anti-rOat5 antibody or anti-rOat3 antibody at 1:2000 dilution (Kojima et al., 2002). Thereafter, they were rinsed with 0.05 M Tris-buffered saline containing 0.1% Tween 20 and incubated with Envision(+) rabbit peroxidase (DakoCytomation California Inc., Carpinteria, CA) for 30 min. After treatment with diaminobenzidine (0.8 mM; Dojindo Laboratories, Kumamoto, Japan), the sections were counterstained with hematoxylin and examined under a light microscope.

Microdissection of Rat Nephron and Reverse Transcription-Polymerase Chain Reaction. The nephron segments of the rats were microdissected as described previously (Nonoguchi et al., 1986) to obtain the following structures: glomeruli; proximal tubules (S_1, S_2, S_3); medullarly thick ascending limb (MAL) and cortical thick ascending limb; and cortical collecting duct (CCD) and outer and inner medullary collecting ducts. Three glomeruli and 2 mm of each dissected tubule were used for reverse transcription (RT)-polymerase chain reaction (PCR).

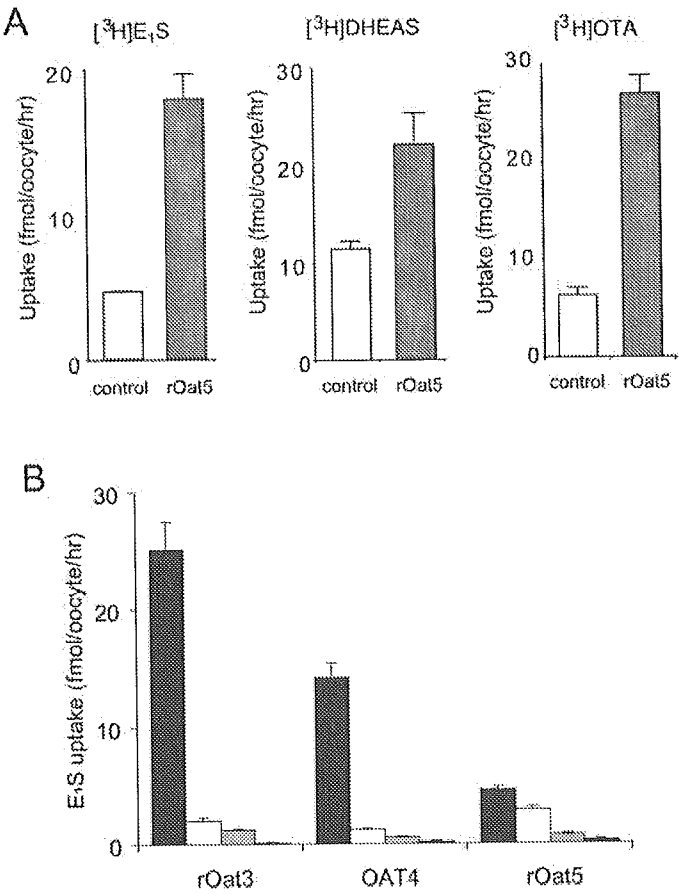

Fig. 1. rOat5-mediated uptake of organic anions. A, the uptake rates of radiolabeled compounds (E_1S, 100 nM; DHEAS, 100 nM; and OTA, 100 nM) by control oocytes (open column) and rOat5-expressing oocytes (closed column) for 1 h were measured (mean ± S.E.M.; n = 8–10). B, direct comparison of representative substrate E_1S transport mediated by rOat3, OAT4, and rOat5. The uptake rates of [^{3}H]E_1S (100 nM) by rOat3, OAT4, and rOat5-expressing oocytes were determined in the absence (closed column) or presence of 5 μM (open column), 50 μM (gray column), and 500 μM (dotted column) unlabeled E_1S.

RT-PCR was performed using a cDNA synthesis kit and a PCR master kit as described previously (Ikebe et al., 2001). Specific primers for rOat3 and rOat5 were designed as follows: rOat3 sense primer, 5′-CCA GTC TTC CCA ATG ACA CCC AGA GG-3′, and antisense primer, 5′-CCA GAT AGA ACC AGC CAG CGT ATG GA-3′; and rOat5 sense primer, 5′-GGG AGG AAG TTC ATT GTG-3′, and antisense primer, 5′-GCA CAC CAC ACC ATA GAG-3′. The cDNA products of rOat3 and rOat5 were 556 and 656 base pairs in length, respectively.

Results

By the EST database search, we found one EST (GenBank accession number AI058341) whose translated amino acid sequence is highly homologous to OAT1, OAT2, OAT3, and OAT4. A rat kidney cDNA library was screened using the corresponding cDNA clone I.M.A.G.E. ID No. UI-*R*-C1-kn-d-03-0-UI as a probe, and cDNA encoding a membrane protein that represents the rat ortholog of the recently identified rOat5 was isolated. rOat5 cDNA consisted of 1995 base pairs encoding a 551-amino acid protein (GenBank/EBI Data Bank with accession number AB051836). rOat5 showed amino acid

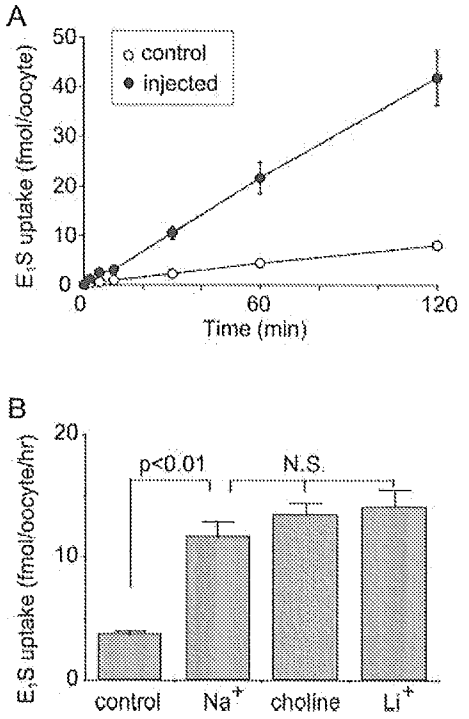

Fig. 2. Transport properties of E_1S via rOat5. A, the rates of uptake of 100 nM [^{3}H]E_1S by control oocytes (open circle) and rOat5-expressing oocytes (closed circle) were measured after 2 h of incubation. B, effect of extracellular cations on [^{3}H]E_1S uptake in *X. laevis* oocytes expressing rOat5. The rate of [^{3}H]E_1S (100 nM) uptake by control (open column) or rOat5-expressing (closed column) oocytes for 1 h was measured (mean ± S.E.M.) in the presence or absence of extracellular Na^+. Extracellular Na^+ was replaced with lithium or choline of equimolar concentration. N.S., not significant.

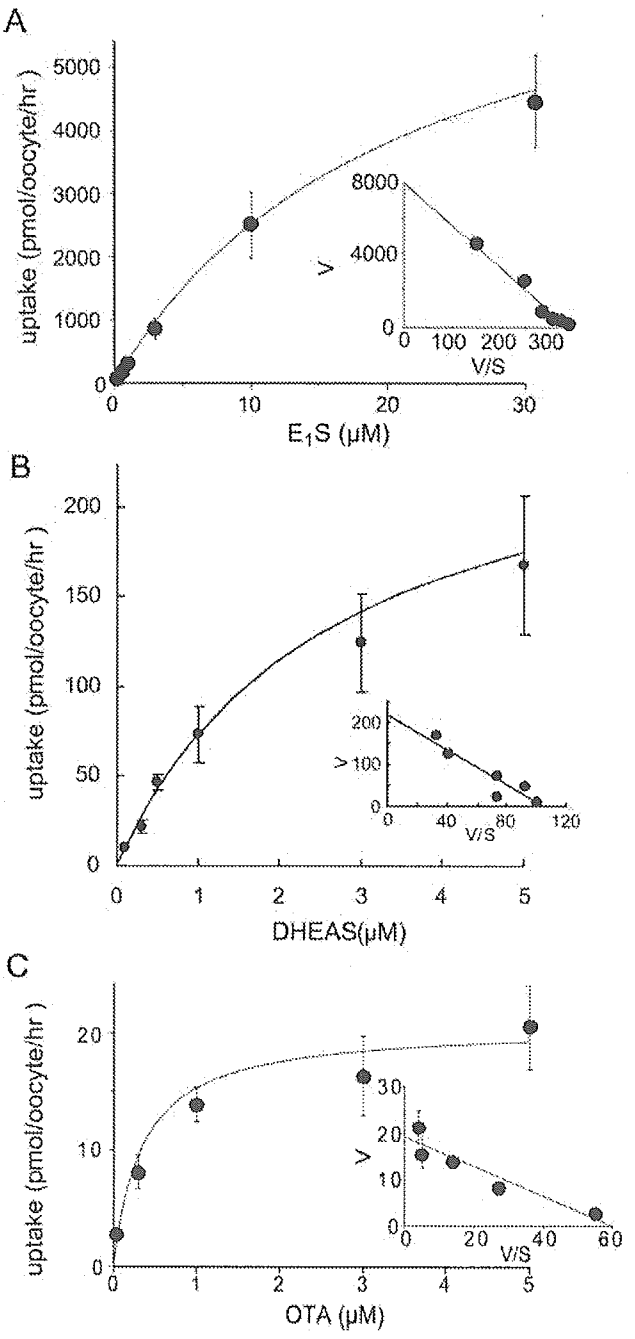

Fig. 3. Representative rates of concentration-dependent uptake of [^{3}H]E_1S (A), [^{3}H]DHEAS (B), and [^{3}H]OTA (C) via rOat5. The rates of uptake of E_1S, DHEAS, and OTA at various concentrations by control or rOat5-expressing oocytes for 1 h were measured (mean ± S.E.M.; n = 8–10). rOat5-mediated transport was determined by subtracting transport velocity for control oocytes from that for rOat5-expressing oocytes. Each value represents the mean ± S.E.M. (n = 8–10) from one typical experiment of three separate experiments.

sequence identities of 39% to rat Oat1 (Sekine et al., 1997; Sweet et al., 1997), 37% to rat Oat2 (Sekine et al., 1998b) and rat Oat3 (Kusuhara et al., 1999), 47% to human OAT4 (Cha et al., 2000), and 44% to a recently cloned OAT member, human urate/anion exchanger URAT1 (Enomoto et al., 2002). rOat5 is obviously not the ortholog of the human OAT5 (hOAT5) (Sun et al., 2001). Kyte-Doolittle hydropathy plot analysis (Kyte and Doolittle, 1982) predicted 12-membrane-spanning domains in rOat5 (hydropathy plot not shown). As in the case for members of the OAT and OCT families, *N*-glycosylation (residues 39, 56, 62, and 102) and protein kinase C-dependent phosphorylation (residues 216, 272, 279, 313, and 536) sites were predicted on the basis of the rOat5 sequence.

Using the *X. laevis* oocyte expression system, we investigated the transport of organic anions by rOat5 (Fig. 1). The uptake rates of [^{3}H]E_1S, [^{3}H]DHEAS, and [^{3}H]OTA in oocytes expressing rOat5 were 2- to 4-fold higher than those in control oocytes (Fig. 1A). rOat5 did not show any uptake of PAH (a representative substrate of OAT1), urate, salicylate, prostaglandins E_2 and $F_2\alpha$, estradiol-17β-glucuronide, and tetraethylammonium (data not shown). To directly compare the transport rates of rOat5 with other renal OATs, we performed uptake studies of E_1S, one of the representative substrates for OATs, with or without unlabeled E_1S using rOat3-, OAT4-, and rOat5-expressing oocytes. As shown in Fig. 1B, although E_1S uptake via rOat5 was strongly inhibited by 50 and 500 μM cold E_1S, its rate of uptake was smaller than the rates of rOat3 and OAT4. In addition, the inhibition by 5 μM E_1S to Oat5-mediated uptake was weak, whereas 5 μM E_1S strongly inhibited rOat3 and OAT4-mediated uptake.

Figure 2 shows the properties of E_1S transport via rOat5. The cell-associated count of [^{3}H]E_1S increased linearly until 2 h of incubation in rOat5-expressing oocytes. This result indicates that rOat5 not only binds but also translocates E_1S into the cytoplasm (Fig. 2A). The rate of E_1S uptake via

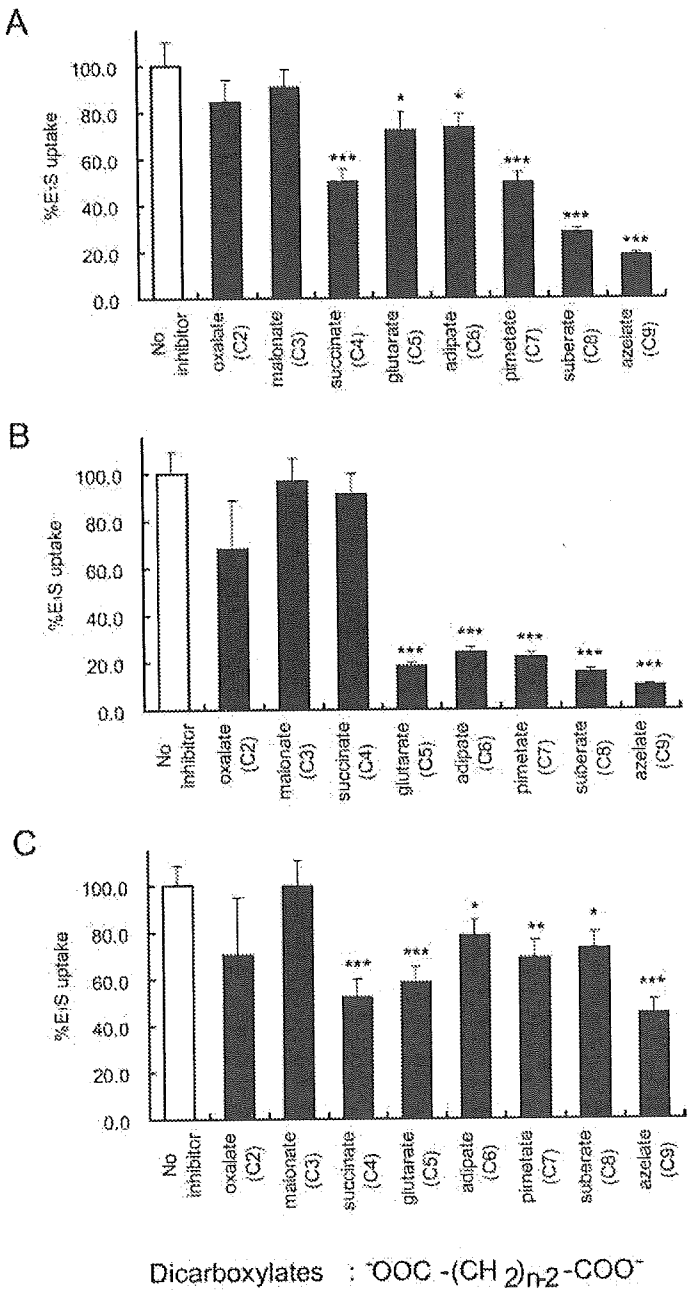

Fig. 4. Inhibition of [^{3}H]E_1S uptake via rOat5 (A), rOat3 (B), and OAT4 (C) by dicarboxylates. The [^{3}H]E_1S concentration used was 100 nM. The inhibitor concentration was 1 mM (gray column). The value was expressed as a percentage of [^{3}H]E_1S uptake for 1 h in rOat5-, rOat3-, or OAT4-expressing oocytes in the absence of the inhibitor (open column) (mean ± S.E.M.; n = 8–10). *, $p < 0.05$; **, $p < 0.01$; ***, $p < 0.001$.

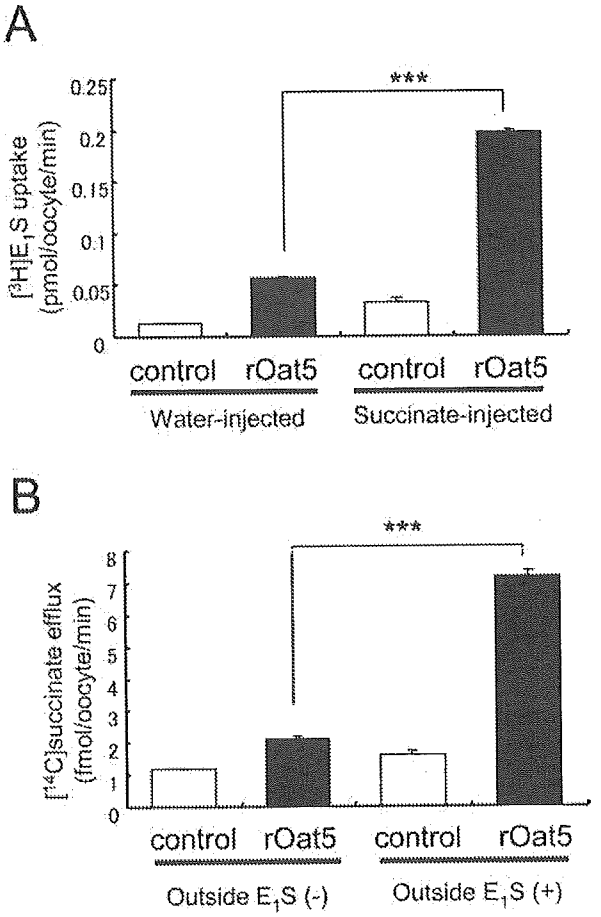

Fig. 5. *trans*-Stimulatory effect on rOat5-mediated transport in *X. laevis* oocytes. A, *trans*-stimulatory effect on the uptake of [^{3}H]E_1S via rOat5. Control (open column) and rOat5-expressing (solid column) oocytes were injected (50 nl) with 50 mM unlabeled succinate (right two lanes) or water (left two lanes) and incubated for 1 h at room temperature. Then, the oocytes were incubated with [^{3}H]E_1S (100 nM), and the amount of [^{3}H]E_1S accumulated for 1 h was determined. B, *trans*-stimulatory effect on the efflux of [^{14}C]succinate via rOat5. Control (open column) and rOat5-expressing (hatched column) oocytes were injected (50 nl) with [^{14}C]succinate (~2 mM). After washing, the oocytes were incubated at room temperature for 1 h and then incubated with 0.1 mM unlabeled E_1S (right lanes) or without a substrate (left lanes) and the amount of [^{14}C]succinate effluxed for 1 h was determined. Each value represents the mean ± S.E.M. (n = 8–10) from one typical experiment of two separate experiments. ***, $p < 0.001$.

rOat5 was not affected by the replacement of extracellular sodium with lithium or choline (Fig. 2B).

We then examined the concentration-dependent uptake of [^{3}H]E_1S, [^{3}H]DHEAS, and [^{3}H]OTA via rOat5 (Fig. 3). The rOat5-mediated uptake of these three compounds manifested saturable kinetics and followed the Michaelis-Menten equation. Eadie-Hofstee equation yielded K_m values of 18.9 ± 3.9, 2.3 ± 0.2, and 0.34 ± 0.06 μM and V_{max} values of 6.6 ± 1.2, 0.25 ± 0.03, and 0.26 ± 0.05 pmol/oocyte/h for E_1S, DHEAS, and OTA, respectively, which were determined using the same batch of oocytes.

Recently, we have reported that OAT4, which is expressed at the apical membrane of human renal proximal tubules, mediates organic anion transport in exchange for five-carbon (C5) dicarboxylate glutarate (Ekaratanawong et al., 2004). These results indicate that OAT4 is an organic anion/dicarboxylate exchanger similar to the basolateral membrane isoforms OAT1 (Sekine et al., 1997; Sweet et al., 1997) and OAT3, which have been clarified as organic anion/dicarboxylate exchangers (Bakhiya et al., 2003; Sweet et al., 2003). To investigate the possibility that rOat5 functions as an organic anion/dicarboxylate exchanger and to search the candidate(s) for its counterion, we first examined the interaction of several dicarboxylates with rOat5, although agents that inhibit are not always exchanged. We performed inhibition experiments in which the uptake of 100 nM [^{3}H]E_1S was measured in the presence of various dicarboxylates (1 mM) ranging from C2 oxalate to C9 azelate (Ullrich et al., 1987). Among these, C3 to C5 dicarboxylates exist as endogenous organic anions in the cells. rOat5-mediated [^{3}H]E_1S uptake was in-

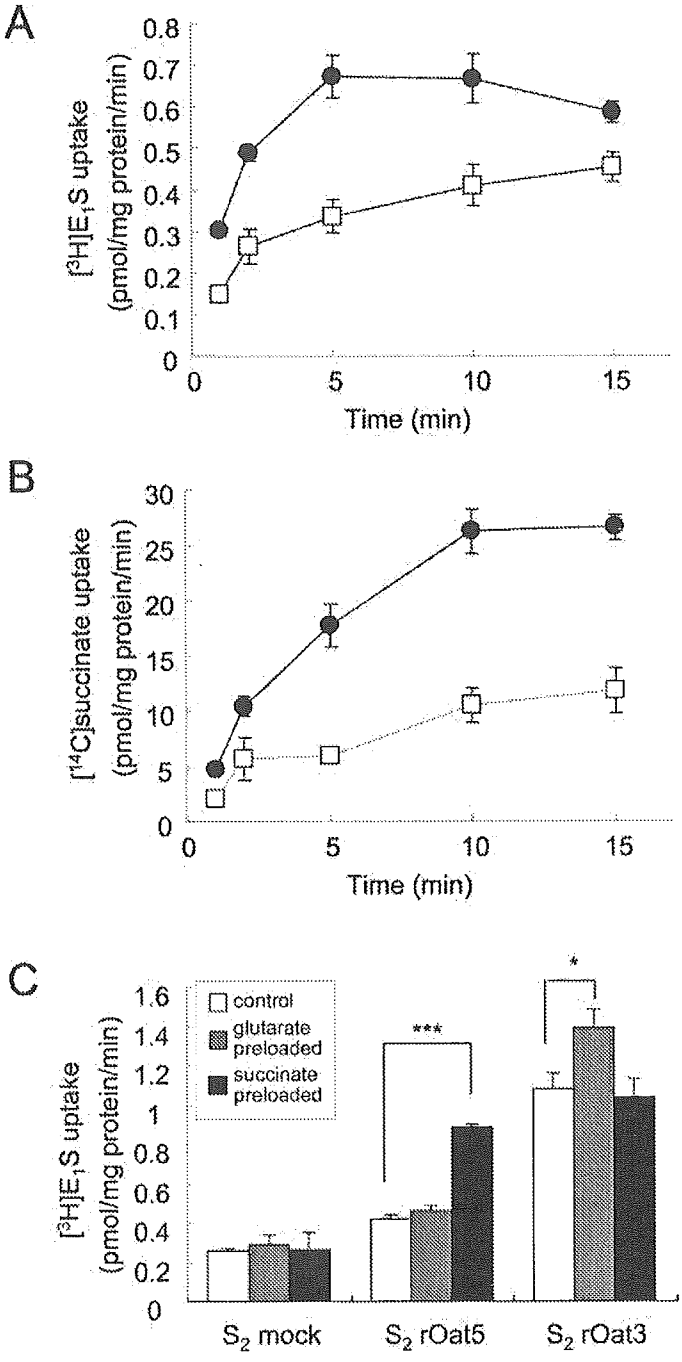

Fig. 6. Transport of E_1S and succinate in S_2 cells expressing OATs. Representative studies of the uptake of 100 nM [^{3}H]E_1S (A) and 10 μM [^{14}C]succinate (B) in rOat5-expressing S_2 cells (S_2 rOat5) (closed circles) and in S_2 cells transfected with the expression vector pcDNA3.1 alone (S_2 mock) (open squares). The cells were incubated for 1 to 15 min at 37°C. C, *trans*-stimulatory effects of succinate and glutarate on rOat5- and rOat3-mediated E_1S transport. The concentrations of preloaded glutarate (gray columns) and succinate (black columns) were 1 mM. Values represent mean ± S.E.M. of two to three independent experiments with four determinations. *, $p < 0.05$; ***, $p < 0.001$.

hibited strongly by succinate (C4) and by all longer dicarboxylates (C7-C9) and moderately by glutarate (C5) and adipate (C6) (Fig. 4A).

To compare the inhibition profiles of other renal OATs, such as the basolateral membrane isoform rOat3 and the apical membrane isoform OAT4, we also performed inhibition experiments using dicarboxylates for E_1S transport in rOat3 and OAT4-expressing oocytes as described above. The basolateral membrane isoform rOat3-mediated [^{3}H]E_1S uptake was inhibited strongly by glutarate (C5) and by all longer dicarboxylates (C6–C9) but not by succinate (C4) (Fig. 4B). In contrast, the apical membrane isoform OAT4-mediated [^{3}H]E_1S uptake was inhibited strongly by succinate (C4), glutarate (C5), and azelate (C9) and moderately by adipate (C6), pimetate (C7), and suberate (C8) (Fig. 4C).

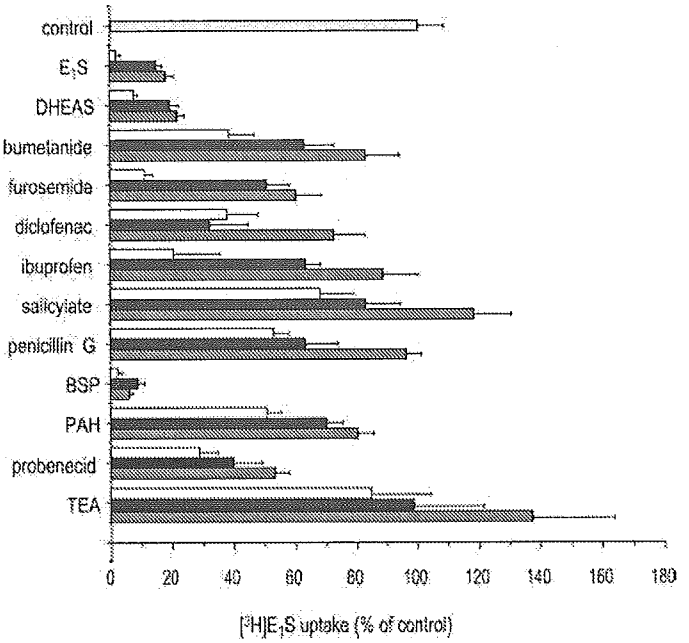

Fig. 7. Inhibition of rOat5-mediated [^{3}H]E_1S uptake by various compounds. The rate of [^{3}H]E_1S (100 nM) uptake by rOat5-expressing or noninjected oocytes was determined in the absence or presence of 50 μM (gray column), 100 μM (closed column), and 500 μM (open column) inhibitors. The value was expressed as a percentage of [^{3}H]E_1S uptake by rOat5-expressing oocytes in the absence of the inhibitor (mean ± S.E.M.; n = 8–10).

Then, we tested the *trans*-stimulatory effect of succinate and E_1S on the uptake and efflux of radiolabeled substrates via rOat5. We injected the unlabeled anionic compounds directly into the oocytes as previously described (Enomoto et al., 2002). The uptake of [^{3}H]E_1S was significantly *trans*-stimulated by unlabeled succinate injected into the oocytes (Fig. 5A), and the efflux of injected [^{14}C]succinate was significantly *trans*-stimulated by unlabeled E_1S in the medium (0.1 mM) (Fig. 5B).

To confirm the succinate transport via rOat5 and the *trans*-stimulatory effect of succinate on rOat5-mediated E_1S transport, we established the cells stably expressing rOat5 (S_2 rOat5). The expression of rOat5 was detected by Western blot analysis using the crude membrane fractions from S_2 rOat5 cells and not from S_2 mock cells (data not shown). Figure 6, A and B, shows the time profiles of the rates of uptake of [^{3}H]E_1S (A) and [^{14}C]succinate (B) by S_2 rOat5 and S_2 mock. Their rates of uptake by S_2 rOat5 were greater than those of S_2 mock and increased linearly until 2 min of incubation. A similar [^{14}C]succinate uptake by S_2 OAT4 cells has recently been identified (N. Anzai, unpublished observation). The uptake of [^{3}H]E_1S via rOat5 was significantly *trans*-stimulated by preloaded succinate (5 mM) (Fig. 6C). In contrast, the uptake of [^{3}H]E_1S via rOat3 was *trans*-stimulated

by preloaded glutarate (5 mM), but not by preloaded succinate (5 mM) (Fig. 6C). On the other hand, similar to a previous report on S_2 OAT4 cells (Ekaratanawong et al., 2004), the uptake of [^{14}C]succinate was not *trans*-stimulated by preloaded E_1S and the efflux of preloaded [^{3}H]E_1S was not stimulated with unlabeled succinate in the medium (5 mM) (data not shown).

To further investigate the substrate selectivity of rOat5, an inhibition study was performed using rOat5-expressing oocytes. The *cis*-inhibitory effect of various compounds at 50, 100, and 500 μM on rOat5-mediated [^{3}H]E_1S (100 nM) uptake was investigated (Fig. 7). Unlabeled E_1S, DHEAS, and sulfobromophthalein at 50 μM each showed a definite inhibitory potency. Bumetanide, furosemide, diclofenac, ibuprofen, and probenecid showed a moderate but dose-dependent inhibitory effect. Salicylate, penicillin G, and PAH showed a much weaker inhibitory effect. In contrast, tetraethylammonium (an organic cation) did not show any inhibitory effect on rOat5-mediated [^{3}H]E_1S uptake.

The interaction of rOat5 with several sulfate and glucuronide conjugates was also examined (Fig. 8). Unlabeled E_1S, DHEAS, 4-methylumbelliferyl sulfate, and β-estradiol sulfate showed a strong inhibitory effect on the rOat5-mediated uptake of [^{3}H]E_1S, whereas *p*-nitrophenyl sulfate and vinblastine sulfate did not (Fig. 8A). In contrast, we could not find the strong inhibitors in all of the glucuronide conjugates tested, which are the well known substrates for OATPs and MRPs (Fig. 8B).

To determine the localization of rOat5 in the kidney compared with rOat3, we immunostained serial kidney sections with the anti-rOat5 and anti-rOat3 antibodies. First of all, to ascertain the specificity of the anti-rOat5 antibody, crude membrane fractions of transfected HEK293 cells were examined. Single band of ~65 kDa was detected in HEK293 cells transfected with rOat5 expression vector (Fig. 9A, lane 1), but no band was detected in cells transfected with vector alone (pcDNA3.1) (Fig. 9A, lane 2). We then examined the expression of rOat5 in rat kidney by diaminobenzidine reaction. Low-magnification light microscopy of 2-μm-thick paraffin sections demonstrated that there is a specific immunostaining for rOat5 in proximal tubular cells, mainly in the outer stripe of the outer medulla as well as in the medullary ray of the cortex (Fig. 9B). No immunostaining for rOat5 was detected in the inner medulla and inner stripe of the outer medulla. In contrast, the broad distribution of rOat3 was detected in tubules from the inner medulla to the cortex, as reported previously (Kojima et al., 2002). rOat3 signals in proximal tubular cells were stronger in the cortical labyrinth than in the medullary ray (Fig. 9C). Under a high magnification, rOat5 immunostaining was detected mainly at the apical membrane of proximal straight tubules (S_3) (Fig. 9D), whereas rOat3 signals were observed mainly at the basolateral membrane of proximal convoluted tubules (S_2) (Fig. 9E). In the corticomedullary junction, the overlapping expressions of apical membrane rOat5 and basolateral membrane rOat3 were detected in some proximal tubular cells (Fig. 9, D and

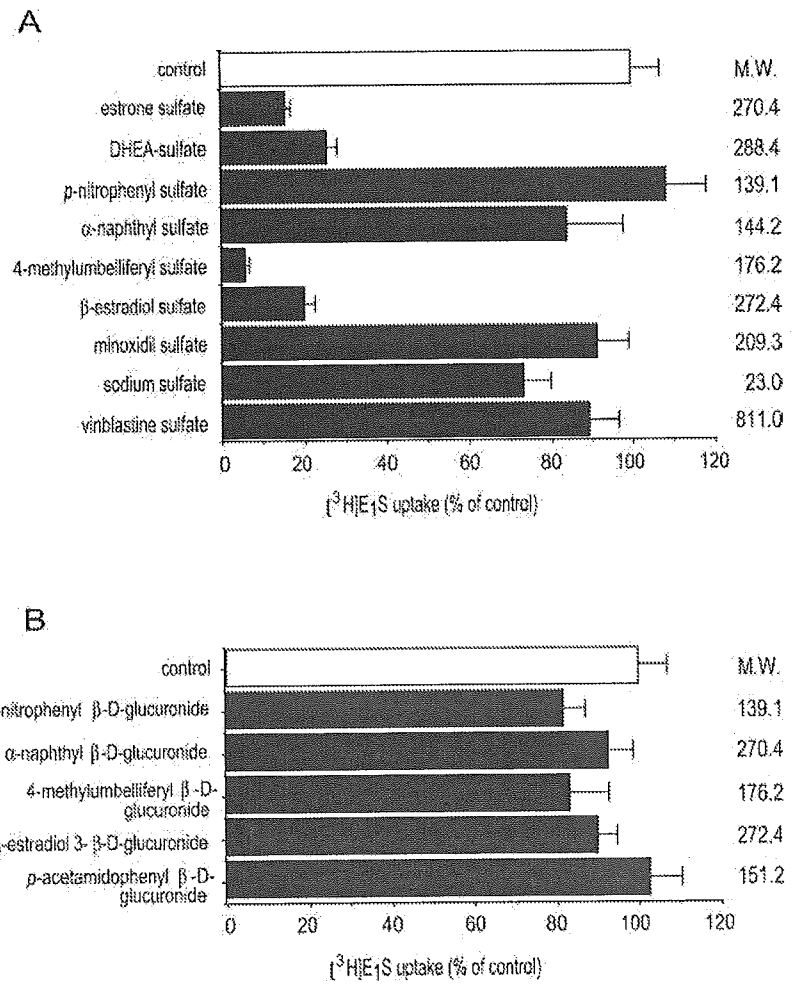

Fig. 8. Inhibition of rOat5-mediated [^{3}H]E_1S uptake by sulfate and glucuronide conjugates. The [^{3}H]E_1S concentration used was 100 nM. The inhibitor concentration was 100 μM. The value was expressed as a percentage of [^{3}H]E_1S uptake in rOat5-expressing oocytes in the absence of the inhibitor (mean ± S.E.M.; n = 8–10).

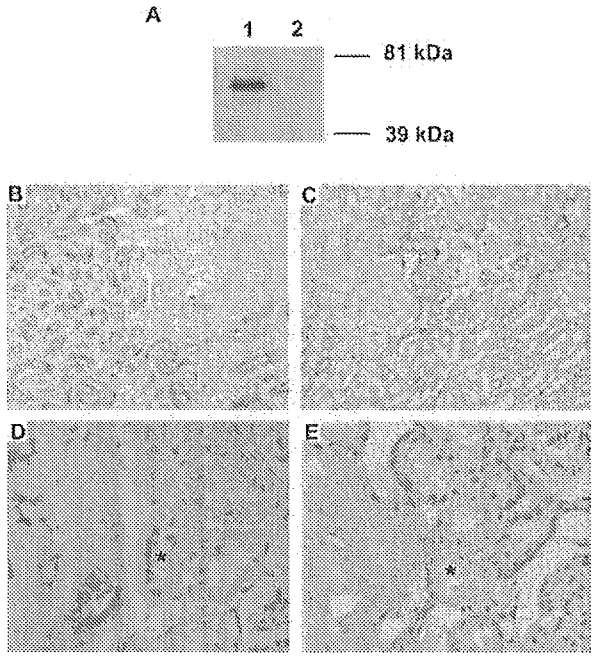

Fig. 9. Immunohistochemical analysis of rOat5 and rOat3 in serial sections of rat kidney. A, Western blot analysis of rOat5 protein. Membrane proteins prepared from HEK293 cells transfected with pcDNA3.1-rOat5 (10 μg) (lane 1) and empty vector (pcDNA3.1) (10 μg) (lane 2) were electrophoresed on a 10% SDS-polyacrylamide gel. Proteins were detected using an enhanced chemiluminescence system. B to E, immunohistochemical labeling of rOat5 and rOat3 by diaminobenzidine reaction of rat kidney tissue cryosections. B, rOat5 was detected in proximal tubules, in the outer stripe of the outer medulla, and in juxtamedullary cortex. C, rOat3 was present in the proximal tubules and tubules in the outer and inner medullae. The apical membrane of proximal tubule was immunostained with the anti-rOat5 antibody (D) and no immunostaining was observed in the basolateral membrane and glomeruli. rOat3 was detected in the basolateral membrane of proximal tubules. E, in some tubules, the overlapping expressions of both rOat3 and rOat5 were observed. *, location of the same renal tubule in serial kidney sections. These figures are representative of typical section samples. Magnifications, ×100 (B, C) and ×400 (D, E).

E). The specificity of the anti-rOat5 antibody was confirmed by the reduced immunoreactivity followed by the preincubation of the antibody with the synthetic rOat5 peptide (200 μg/ml) (data not shown).

In addition, we performed RT-PCR analysis to determine the intranephron distributions of rOat5 and rOat3 mRNAs. rOat5 mRNA was expressed strongly in the S_2 and S_3 segments of the proximal tubule, moderately in glomeruli and CCD, and weakly in MAL. rOat3 mRNA was expressed strongly in the S_1 and S_2 segments of the proximal tubule, moderately in the S_3 segment, and weakly in MAL and collecting ducts. The overlapping expressions of rOat5 and rOat3 were observed in the S_2 and S_3 segments (Fig. 10).

Discussion

In this study, we identified, for the first time, the four-carbon dicarboxylate succinate (C4) as one of the counterions for the OAT family as shown in Figs. 4A, 5, and 6. It has been established that the classical renal organic anion transport system at the basolateral membrane uses five-carbon dicarboxylate α-ketoglutarate (C5) as a counterion for its organic anion exchange (Burckhardt et al., 2001). The first identified that OAT family members OAT1 and fROAT are PAH/α-ketoglutarate exchangers (Sekine et al., 1997; Sweet et al., 1997; Wolff et al., 1997). Recently, rat and human OAT3s have been shown to be organic anion/α-ketoglutarate exchangers as well (Bakhiya et al., 2003; Sweet et al., 2003). To date, there have been no reports regarding the role of succinate as a counterion for renal organic anion transporters. In a previous study, Youngblood and Sweet (2004) reported that the mOat5-mediated transport was neither *cis*-inhibited nor *trans*-stimulated by the dicarboxylate glutarate and succinate. As we previously discussed in our report on OAT4, 500 μM glutarate is not sufficient to inhibit the OAT4-mediated transport and the preincubation of dicarboxylates is not suitable for inducing the *trans*-stimulatory effect in oocyte system (Ekaratanawong et al., 2004). Therefore, in this study, we used 1 mM succinate, which is 4-fold higher than that used by Youngblood and Sweet, and we directly injected cold succinate into the oocytes instead of using the preincubation method they used for mouse Oat5. These modifications might lead to the identification of the organic anion/succinate exchange property of rOat5.

It was reported that glomerular-filtrated α-ketoglutarate is abundantly reabsorbed from the lumen in the early segments of proximal tubules (Ferrier et al., 1985) and that a portion of this reabsorbed α-ketoglutarate is considered to contribute to the basolateral uptake of organic anions via organic anion/α-ketoglutarate exchangers, such as OAT1 and OAT3 (Burckhardt and Pritchard, 2000). However, our previous report indicated that organic anion/α-ketoglutarate exchange activity exists not only in the basolaterally localized OAT1 and OAT3 but also in the apically localized OAT4 of the same proximal tubular cells (Ekaratanawong et al., 2004). As Schmitt and Burckhardt (1993) discussed in the case of bovine BBMVs , it seems unlikely that two exchangers with the same properties existing on both sides of membranes accomplish the vectorial transport of organic anions. However, our current finding that succinate is the most likely counterion for the rOat5-mediated transport may explain this contradiction. To separate or isolate the transport of organic anions at the apical membrane of proximal tubules from that at the basolateral membrane, the apical membrane isoforms of OAT seem to use four-carbon dicarboxylate succinate as a counterion, whereas the basolateral membrane OAT isoforms use five-carbon dicarboxylate as a counterion (Fig. 11). This idea is supported by the results shown in Fig. 4, B and C, that the basolateral membrane isoform rOat3-mediated transport was inhibited strongly by glutarate, but not by succinate, and that the apical membrane isoform OAT4-mediated transport was inhibited by succinate as well as glutarate. It is noteworthy that urate transport via the urate/anion exchanger URAT1 localized at the renal apical membrane was also inhibited by succinate at a millimolar concentration in the *X. laevis* oocyte system (Enomoto et al., 2002). It has been suggested that the succinate exchange property is a common mechanism for the apical membrane isoforms of OAT family members.

Dicarboxylic and tricarboxylic acids are actively taken up by proximal tubular cells from both peritubular fluid and glomerular filtrate (Simpson, 1983). The transport processes have been assumed to be mediated by two distinct Na^+-dicarboxylate pathways, the luminal and the basolateral membrane Na^+-dicarboxylate transporters, NaDC1 and NaDC3 (Wright, 1985; Wright and Wunz, 1987). One proposed function of these two transporters is to supply Krebs

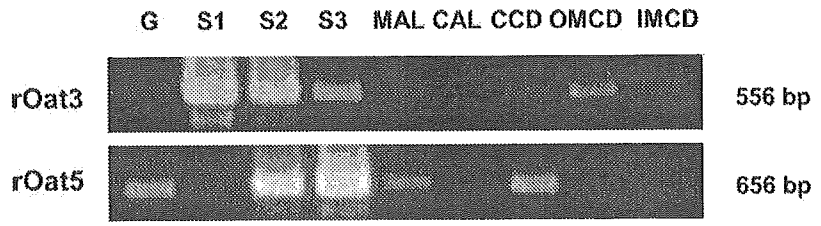

Fig. 10. Intranephron distribution of rOat5 and rOat3 in rat kidney. rOat5 mRNA was expressed strongly in the S_2 and S_3 segments of proximal tubules, moderately in glomeruli and CCD, and weakly in MAL (top panel). rOat3 mRNA was expressed strongly in the S_1 and S_2 segments of proximal tubules, moderately in the S_3 segment, and weakly in MAL and collecting ducts (bottom panel).

cycle intermediates, such as citrate, α-ketoglutarate, and succinate, to support the oxidative metabolism in proximal tubular cells. Another function that has been proposed is to sustain the outward dicarboxylate gradient that drives the organic anion uptake into proximal tubular cells. Because α-ketoglutarate is the most abundant within a proximal tubular cell (~200 μM) and is found in blood circulation with mean plasma level of ~10 μM (Pritchard, 1995), α-ketoglutarate is considered to be the most likely candidate for the physiological counterion participating in organic anion transport, particularly at the basolateral membrane. However, succinate has recently been identified by He et al. (2004) as a natural ligand for GPR91, an orphan G-protein-coupled receptor in the proximal and distal tubules. They showed that succinate increases blood pressure in mice and that the succinate-induced hypertension involves the renin-angiotensin system. Succinate is also found in blood circulation with a mean plasma level of ~5 μM (Kushnir et al., 2001). These findings raise the possibility that succinate level surrounding proximal tubular cells, determined by the balance between the uptake of dicarboxylates via NaDCs and its efflux via OATs, is an important factor that regulates renovascular hypertension. Succinate is a prototypical substrate of NaDCs, and it is also reabsorbed in proximal tubules with α-ketoglutarate. It is noteworthy that the apical membrane isoform of this transporter NaDC1 is expressed in the S_2 and S_3 segments in rats (Sekine et al., 1998a) and that this distribution profile is similar to that of rOat5 (Figs. 9 and 10). These results raise another possibility that rOat5 participates in the dicarboxylates efflux (including succinate) from tubular cells using the outward dicarboxylate gradient in the tubular cells.

rOat5 is unique among OATs in several respects. rOat5 is functionally distinct from OAT4 in substrate specificity, affinity, and intranephron localization. First, rOat5 did not transport PAH (data not shown), although one of the common characteristics of the four OAT isoforms (OAT1 to OAT4) identified to date is the transport of PAH, a prototypical substrate for renal organic anion transport. In particular, OAT1 is considered to be a classical PAH transporter because it mediates the high-affinity transport of PAH in exchange for intracellular α-ketoglutarate (Burckhardt et al., 2001). The lack of PAH recognition by rOat5 seems to be one reason that the apical organic anion/dicarboxylate-exchange system was not found by previous classical transport studies using isolated rat renal tubules or brush-border membrane vesicles preparation. Second, the affinity for E_1S transport is different between rOat5 and other OAT members. As reported previously, both OAT3 and OAT4 manifested a high affinity for E_1S. K_m for E_1S transport for rOat3 was 2.3 μM (Kusuhara et al., 1999), that for hOAT3 was 3.1 μM (Cha et al., 2001), and that for OAT4 was 1.01 μM (Cha et al., 2000). On the other hand, K_m for E_1S transport for rOat5 was 18.9 μM, which was approximately 10- to 20-fold higher than that by

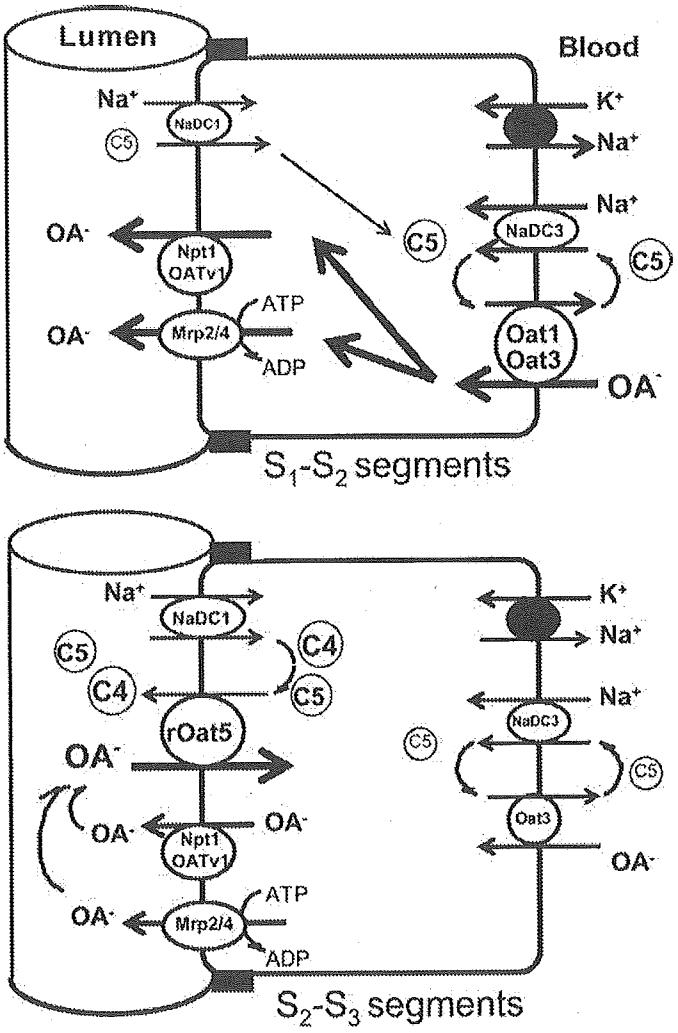

Fig. 11. Proposed scheme of organic anion (OA^-) transport in rodent renal proximal tubules. In the early (S_1 to S_2) segments of the proximal tubules (top), OAs, including xenobiotics (e.g., PAH), enter into proximal tubular cells via basolateral Oat1 and/or Oat3 using the outward gradient of α-ketoglutarate (C5) created by NaDC3 and they are secreted into the urine via apical efflux transporters, such as Mrp2/4 and Npt1(OAT_V1). In contrast, in the late (S_2 to S_3) segments of the proximal tubules (bottom), because the apical membrane rOat5 expression level is high and the basolateral membrane Oat3 expressions level is low, some organic anions, such as steroid sulfates that are glomerular filtrated or tubular secreted or effluxed by Mrp2/4 and/or Npt1(OAT_V1), are reabsorbed by rOat5 using the outward gradient of succinate (C4) and α-ketoglutarate (C5) generated by NaDC1. Some organic anions may be accumulated into proximal tubular cells and may induce xenobiotic-induced nephrotoxicity.

other OATs (Fig. 3). Third, rOat5 was expressed mainly in the late segments (S_2 and S_3) of proximal tubules (Figs. 9 and 10). On the other hand, another renal apical membrane OAT isoform OAT4 was expressed throughout the proximal tubules (from S_1 to S_3) (Ekaratanawong et al., 2004). It is noteworthy that our previous study demonstrated that OAT4 immunoreactivities completely overlap with those of OAT1 and OAT3 in the S_1 and S_2 segments of proximal tubules (Ekaratanawong et al., 2004), whereas rOat5 immunoreactivity overlapped partly with that of rOat3 (Fig. 9).

As described above, rOat5 shows a remote amino acid sequence similarity to OAT4 (47%) and it appears to be different from OAT4. However, rOat5 still shares some common characteristics with other OATs. rOat5, similar to OAT3 and OAT4, and exhibits narrow substrate selectivity for sulfate conjugates (Fig. 8) (Kusuhara et al., 1999; Cha et al., 2000). The inhibition study revealed that the pharmacological profile of rOat5 is similar to that of OAT3 and OAT4 in which rOat5-mediated E_1S uptake was inhibited by bumetanide, furosemide, penicillin G, probenecid, and sulfobromophthalein (Fig. 7). Furthermore, the inhibition profile of rOat5 for sulfate and glucuronide conjugates was similar to that of OAT4 (Fig. 8). rOat5 preferentially accepted sulfate conjugates rather than glucuronide conjugates, whereas it did not accept small sulfoconjugates, such as *p*-nitrophenyl sulfate (molecular weight: 257.3), and large sulfoconjugates, such as vinblastine sulfate (molecular weight: 909.1). Therefore, it will be interesting to determine the common inherent structural traits responsible for such similar substrate selectivities of different transporters.

In summary, we describes the intrarenal localization and the functional characterization of an organic anion transporter rOat5 (*Slc22a19*). The observations in this study suggest that the renal apical transporter rOat5 functions as an apical backflux pathway (Ekaratanawong et al., 2004) for organic anions (e.g., sulfate conjugates) in the terminal segment of renal proximal tubules, driven by an outward gradient of succinate under physiological conditions (Fig. 11). rOat5 may contribute to selectively reabsorb sulfate conjugates excreted into luminal fluid by the apical organic anion efflux transporters (e.g., MRP2/4 and NPT1/OAT_V1) in the early segment of renal proximal tubules. Although the relative contribution of rOat5 to renal organic anion and/or dicarboxylate handling needs to be clarified, this study provides new insights into the functional basis and the integration of the apical transport pathway of organic anions, including xenobiotics and endogenous compounds as well as dicarboxylates, such as succinate, in the rat kidneys.

Acknowledgments

We thank A. Toki for technical assistance and Drs. A. Bahn, A. M. Torres, and T. Sekine for helpful discussions. The anti-rOat5 and anti-rOat3 polyclonal antibodies were supplied by Transgenic Inc. (Kumamoto, Japan).

References

Anzai N, Miyazaki H, Noshiro R, Khamdang S, Chairoungdua A, Shin HJ, Enomoto A, Sakamoto S, Hirata T, Tomita K, et al. (2004) The multivalent PDZ domain-containing protein PDZK1 regulates transport activity of renal urate-anion exchanger URAT1 via its C terminus. *J Biol Chem* **279:**45942–45950.

Bakhiya N, Bahn A, Burckhardt G, and Wolff NA (2003) Human organic anion transporter 3 (hOAT3) can operate as an exchanger and mediate secretory urate flux. *Cell Physiol Biochem* **13:**249–256.

Burckhardt G and Pritchard JB (2000) Organic aion and cation antiporters, in *The Kidney Physiology and Pathophysiology, 3rd Editions* (Seldin DW and Giebisch G, eds) pp 193–222, Lippincott Williams & Wilkins, Philadelphia

Burckhardt G, Bahn A, and Wolff NA (2001) Molecular physiology of renal *p*-aminohippurate secretion. *News Physiol Sci* **16:**114–118.

Cha SH, Sekine T, Fukushima J-I, Kanai Y, Kobayashi Y, Goya T, and Endou H (2001) Identification and characterization of human organic anion transporter 3 expressing predominantly in the kidney. *Mol Pharmacol* **59:**1277–1286.

Cha SH, Sekine T, Kusuhara H, Yu E, Kim JY, Kim DK, Sugiyama Y, Kanai Y, and Endou H (2000) Molecular cloning and characterization of multispecific organic anion transporter 4 expressed in the placenta. *J Biol Chem* **275:**4507–4512.

Ekaratanawong S, Anzai N, Jutabha P, Miyazaki H, Noshiro R, Takeda M, Kanai Y, Sophasan S, and Endou H (2004) Human organic anion transporter 4 is a renal apical organic anion/dicarboxylate exchanger in the proximal tubules. *J Pharmacol Sci* **94:**297–304.

Enomoto A, Kimura H, Chairoungdua A, Shigeta Y, Jutabha P, Cha SH, Hosoyamada M, Takeda M, Sekine T, Igarashi T, et al. (2002) Molecular identification of a renal urate anion exchanger that regulates blood urate levels. *Nature (Lond)* **417:**447–452.

Ferrier B, Martin M, and Baverel G (1985) Reabsorption and secretion of alpha-ketoglutarate along the rat nephron: a micropuncture study. *Am J Physiol* **248:** F404–F412.

He W, Miao FJ, Lin DC, Schwandner RT, Wang Z, Gao J, Chen JL, Tian H, and Ling L (2004) Citric acid cycle intermediates as ligands for orphan G-protein-coupled receptors. *Nature (Lond)* **429:**188–193.

Ikebe M, Nonoguchi H, Nakayama Y, Tashima Y, and Tomita K (2001) Up-regulation of the secretory-type Na(+)/K(+)/2Cl(−)-cotransporter in the kidney by metabolic acidosis and dehydration in rats. *J Am Soc Nephrol* **12:**423–430.

Jutabha P, Kanai Y, Hosoyamada M, Chairoungdua A, Kim DK, Iribe Y, Babu E, Kim JY, Anzai N, Chatsudthipong V, et al. (2003) Identification of a novel voltage-driven organic anion transporter present at apical membrane of renal proximal tubule. *J Biol Chem* **278:**27930–27938.

Koepsell H and Endou H (2004) The SLC22 drug transporter family. *Pflugers Arch* **447:**666–676.

Kojima R, Sekine T, Kawachi M, Cha SH, Suzuki Y, and Endou H (2002) Immunolocalization of multispecific organic anion transporters, OAT1, OAT2 and OAT3, in rat kidney. *J Am Soc Nephrol* **13:**848–857.

Krick W, Wolff NA, and Burckhardt G (2000) Voltage-driven *p*-aminohippurate, chloride and urate transport in porcine renal brush-border membrane vesicles. *Pfluegers Arch* **441:**125–132.

Kushnir MM, Komaromy-Hiller G, Shushan B, Urry FM, and Roberts WL (2001) Analysis of dicarboxylic acids by tandem mass spectrometry. High-throughput quantitative measurement of methylmalonic acid in serum, plasma and urine. *Clin Chem* **47:**1993–2002.

Kusuhara H, Sekine T, Utsunomiya-Tate N, Tsuda M, Kojima R, Cha SH, Sugiyama Y, Kanai Y, and Endou H (1999) Molecular cloning and characterization of a new multispecific organic anion transporter from rat brain. *J Biol Chem* **274:**13675–13680.

Kyte J and Doolittle RF (1982) A simple method for displaying the hydropathic character of a protein. *J Mol Biol* **157:**105–132.

Nonoguchi H, Takehara Y, and Endou H (1986) Intra- and inter-nephron heterogeneity of ammoniagenesis in rats: effects of chronic metabolic acidosis and potassium depletion. *Pflugers Arch* **407:**245–251.

Pritchard JB (1995) Intracellular alpha-ketoglutarate controls the efficacy of renal organic anion transport. *J Pharmacol Exp Ther* **274:**1278–1284.

Russel FGM, Masereeuw R, and van Aubel RAMH (2002) Molecular aspects of renal anionic drug transport. *Annu Rev Physiol* **64:**563–594.

Schmitt C and Burckhardt G (1993) *p*-Aminohippurate/2-oxoglutarate exchange in bovine renal brush-border and basolateral membrane vesicles. *Pflueg Arch Eur J Physiol* **423:**280–290.

Sekine T, Cha SH, Hosoyamada M, Kanai Y, Watanabe N, Furuta Y, Fukuda K, Igarashi T, and Endou H (1998a) Cloning, functional characterization and localization of a rat renal Na^+-dicarboxylate transporter. *Am J Physiol* **275:**F298–F305.

Sekine T, Cha SH, Tsuda M, Apiwattanakul N, Nakajima N, Kanai Y, and Endou H (1998b) Identification of multispecific organic anion transporter 2 expressed predominantly in the liver. *FEBS Lett* **429:**179–182.

Sekine T, Watanabe N, Hosoyamada M, Kanai Y, and Endou H (1997) Expression cloning and characterization of a novel multispecific organic anion transporter. *J Biol Chem* **272:**18526–18529.

Simpson DP (1983) Citrate excretion: a window on renal metabolism. *Am J Physiol* **244:**F223–F234.

Smeets PH, van Aubel RA, Wouterse AC, van den Heuvel JJ, and Russel FG (2004) Contribution of multidrug resistance protein 2 (MRP2/ABCC2) to the renal excretion of *p*-aminohippurate (PAH) and identification of MRP4 (ABCC4) as a novel PAH transporter. *J Am Soc Nephrol* **15:**2828–2835.

Sun W, Wu RR, van Poelje PD, and Erion MD (2001) Isolation of a family of organic anion transporters from human liver and kidney. *Biochem Biophys Res Commun* **283:**417–422.

Sweet DH, Chan LM, Walden R, Yang XP, Miller DS, and Pritchard JB (2003) Organic anion transporter 3 (Slc22a8) is a dicarboxylate exchanger indirectly coupled to the Na+ gradient. *Am J Physiol* **284:**F763–F769.

Sweet DH, Wolff NA, and Pritchard JB (1997) Expression cloning and characterization of ROAT1. The basolateral organic anion transporter in rat kidney. *J Biol Chem* **272:**30088–30095.

Takeda M, Khamdang S, Narikawa S, Kimura H, Hosoyamada M, Cha SH, Sekine T, and Endou H (2002) Characterization of methotrexate transport and its drug interactions with human organic anion transporters. *J Pharmacol Exp Ther* **302:** 666–671.

Uchino H, Tamai I, Yamashita K, Minemoto Y, Sai Y, Yabuuchi H, Miyamoto K, Takeda E, and Tsuji A (2000) *p*-Aminohippuric acid transport at renal apical

membrane mediated by human inorganic phosphate transporter NPT1. *Biochem Biophys Res Commun* **270:**254–259.
Ullrich KJ, Rumrich G, Fritzsch G, and Kloss S (1987) Contraluminal *para*-aminohippurate (PAH) transport in the proximal tubule of the rat kidney. II. Specificity: aliphatic dicarboxylic acids. *Pflug Arch Eur J Physiol* **408:**38–45.
van Aubel RAMH, Smeets PHE, Peters JGP, Bindels RJM, and Russel FGM (2002) The MRP4/ABCC4 gene encodes a novel apical organic anion transporter in human kidney proximal tubules: putative efflux pump for urinary cAMP and cGMP. *J Am Soc Nephrol* **13:**595–603.
Werner D, Martinez F, and Roch-Ramel F (1990) Urate and *p*-aminohippurate transport in the brush border membrane of the pig kidney. *J Pharmacol Exp Ther* **252:**792–799.
Wolff NA, Werner A, Burkhardt S, and Burckhardt G (1997) Expression cloning and characterization of a renal organic anion transporter from winter flounder. *FEBS Lett* **417:**287–291.
Wright EM (1985) Transport of carboxylic acids by renal membrane vesicles. *Annu Rev Physiol* **47:**127–141.
Wright SH and Dantzler WH (2004) Molecular and cellular physiology of renal organic cation and anion transport. *Physiol Rev* **84:**987–1049.
Wright SH and Wunz TM (1987) Succinate and citrate transport in renal basolateral and brush-border membranes. *Am J Physiol* **253:**F432–F439.
Youngblood GL and Sweet DH (2004) Identification and functional assessment of the novel murine organic anion transporter Oat5 (Slc22a19) expressed in kidney. *Am J Physiol* **287:**F236–F244.

Address correspondence to: Dr. Yoshikatsu Kanai, Department of Pharmacology and Toxicology, Kyorin University School of Medicine, 6-20-2 Shinkawa, Mitaka-shi, Tokyo 181-8611, Japan. E-mail: ykanai@kyorin-u.ac.jp

Carcinogenesis vol.26 no.2 pp.353–357, 2005
doi:10.1093/carcin/bgh322

Prostaglandin E receptor subtype EP_1 deficiency inhibits colon cancer development

Toshihiko Kawamori[3], Tomohiro Kitamura, Kouji Watanabe, Naoaki Uchiya, Takayuki Maruyama[1], Shuh Narumiya[2], Takashi Sugimura and Keiji Wakabayashi*

Cancer Prevention Basic Research Project, National Cancer Center Research Institute, 1-1 Tsukiji 5-chome, Chuo-ku, Tokyo 104-0045, Japan, [1]Minase Research Institute, Ono Pharmaceutical Co. Ltd, Osaka 618-8585, Japan and [2]Department of Pharmacology, Faculty of Medicine, Kyoto University, Kyoto 606-8315, Japan
[3]Present address: Medical University of South Carolina, Pathology and Laboratory Medicine, 165 Ashley Avenue, Suite 309, Charleston, SC 29425, USA

*To whom correspondence should be addressed
Email: kawamori@musc.edu or kwakabay@gan2.ncc.go.jp

Prostaglandin E_2 exerts its biological activity through binding to its membrane receptors, E-prostanoid (EP) $receptors_{1-4}$. Our previous finding that lack of EP_1 receptor inhibits the early stages of colon carcinogenesis led us to investigate whether EP_1 receptor deficiency reduces colon cancer development induced by azoxymethane (AOM) using EP_1 receptor knockout mice. At 6 weeks of age 33 homozygous EP_1-deficient ($EP_1^{-/-}$) mice and 28 wild-type ($EP_1^{+/+}$) mice were given i.p. AOM (10 mg/kg body wt) once a week for 6 weeks. At 56 weeks of age all animals were killed and intestinal tumors were examined. The results clearly indicated that lack of EP_1 receptor significantly reduced colon cancer incidence (27 versus 57%, $P < 0.05$) and multiplicity (0.30 versus 0.76, $P < 0.05$) as well as tumor volume (12.2 versus 75.6 mm^3, $P < 0.05$). In $EP_1^{-/-}$ mice, silver stained nucleolar organization region protein count as cell proliferation marker was significantly reduced (1.35 versus 2.17, $P < 0.001$) and apoptosis was significantly increased (0.685 versus 0.077, $P < 0.001$) in colon tumors induced by AOM compared with those in $EP_1^{+/+}$ mice. We confirmed that EP_1 receptor mRNA was overexpressed in colon cancers of $EP_1^{+/+}$ mice using reverse transcription–polymerase chain reaction. These results provide strong evidence that the EP_1 receptor is of major importance for colon cancer development and it could be a new target for a mechanism-based chemoprevention strategy against colon cancer development.

Introduction

Colon cancer development appears to be closely linked with alterations in the arachidonic acid cascade and non-steroidal anti-inflammatory drugs reduce the risk of colon cancer development in human (1) and the incidence of carcinogen-induced colon cancers in rodents (2) through inhibition of cyclooxygenase (COX) activity. There are two isozymes of COX, referred to as COX-1 and COX-2. COX-2, the inducible form, is known to be overexpressed in colon cancers in rodents (3) and humans (4,5), whereas COX-1 is constitutively expressed and may contribute to various physiological functions. Celecoxib, a selective COX-2 inhibitor, has shown strong chemopreventive effects against colon cancer development in animal models (6,7) and may significantly reduce the numbers of colorectal polyps in familial adenomatous polyposis patients (8). There is accumulating evidence that COX-2 plays a pivotal role in colon carcinogenesis from genetic and pharmacological studies (9,10). Recently, however, there was a report using knockout mice that COX-1 contributed to colon carcinogenesis as well as COX-2 (11). These results suggest that not only COX-2 but also COX-1 contribute to colon carcinogenesis. Several reports have documented increased levels of prostaglandin E_2 (PGE_2), one of the major prostanoids, in colon cancer tissues compared with surrounding normal appearing mucosa of rodents and humans (12,13). Taken together, both COX enzymes and the levels of their product PGE_2 may be important factors and may play roles in colon carcinogenesis. In addition, recent studies provide evidence that PGE_2 administration enhances AOM-induced colon carcinogenesis in male F344 rats (14). Thus, we hypothesized that decreased signaling via the PGE_2 pathway may be associated with inhibition of colon cancer development. PGE_2 exerts its biological activity through binding to the membrane receptors E-prostanoid (EP) $receptors_{1-4}$. Therefore, it is likely that lack of specific receptors may contribute to the inhibitory effects on colon carcinogenesis. Recent development of mice lacking the genes encoding these receptors (15–17) has allowed us to investigate which types of receptors are involved in colon carcinogenesis. In our previous studies, EP_1 or EP_4 receptor deficiency and specific antagonists against these receptors significantly reduced the number of azoxymethane (AOM)-induced aberrant crypt foci, which are thought to be preneoplastic lesions in the colon (18,19). The antagonists also inhibited intestinal polyp formation in *Min* mice, suggesting that receptors EP_1 and EP_4 play important roles in the early stages of colon carcinogenesis. However, the question remains as to whether EP_1 receptor deficiency really has an impact on colon cancer development. Therefore, we designed the present study to analyze the effects of EP_1 receptor deficiency on colon cancer development induced by AOM using knockout mice.

The inhibitory mechanism was investigated by determining cell proliferation and apoptosis in colon tumors. An assessment of EP receptor expression in colonic normal mucosa and cancers of mice with or without EP_1 receptors using the reverse transcription–polymerase chain reaction (RT-PCR) method was also examined. The mouse *EP_1* receptor gene, consisting of three exons, is predominantly expressed in the kidney and in the hypothalamus of the brain. Mouse *PKN*, a newly discovered gene encoding a protein kinase related to the protein

Abbreviations: AgNOR, silver stained nucleolar organizer region protein; AOM, azoxymethane; COX, cyclooxygenase; EP, E-prostanoid; NORs, nucleolar organizer regions; PGE_2, prostaglandin E_2; PKN, protein kinase N; RT-PCR, reverse transcription–polymerase chain reaction.

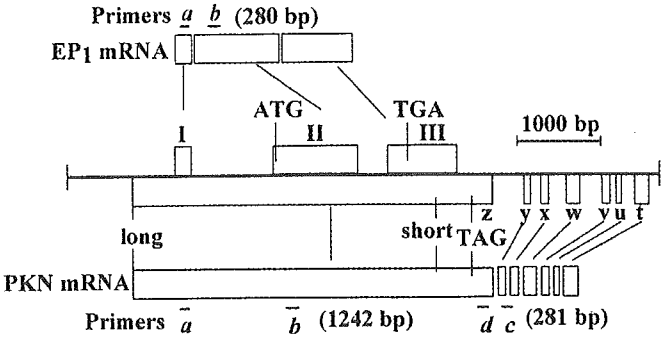

Fig. 1. Gene organization at the mouse EP_1/*PKN* gene locus and the transcripts produced. The center line represents the 7.2 kb of sequenced genomic DNA. Open boxes represent exons. The EP_1 gene exons are numbered I–III and are shown above the line. Under the line are the seven last exons of the *PKN* gene. Solid bars illustrate mRNAs produced at this locus. *a*, *b*, *c* and *d* indicate primer positions within the locus.

kinase C family (20), overlaps the whole EP_1 gene in a tail-to-tail manner (21), indicating that the whole EP_1 gene is contained within the 3′-untranslated region of a long protein kinase N (*PKN*) gene transcript (Figure 1). Our EP_1 knockout mice were made by inserting the neomycin-resistance gene into the FspI site of exon 2, which is located immediately before the sequence encoding the first transmembrane domain (15). Therefore, this EP_1 receptor knockout strategy may influence a long *PKN* gene transcript. In this report, to confirm that the *PKN* gene is not a player in AOM-induced colon carcinogenesis, expression of the *PKN* gene in mice with or without EP_1 receptor was also investigated using the RT-PCR method.

Materials and methods

Animals and chemicals

The mouse gene encoding the EP_1 receptor was disrupted by gene knockout methods using homologous recombination, as reported previously (15). The chimeric mice generated were back-crossed with C57BL/6Cr mice and the resulting wild-type and homozygous mutant males of the F_2 progeny were used at 6 weeks. The genotypes of the knockout mice were confirmed by PCR according to the method described previously (15). The animals were housed in plastic cages at 24 ± 2°C and 55% humidity with a 12 h light/dark cycle and maintained on powder diet (AIN-76A; Dyets Inc., Bethlehem, PA). AOM was purchased from Sigma Chemical Co. (St Louis, MO). The study was performed with the approval of the Institutional Animal Care and Use Committee.

Experimental procedure

At 6 weeks of age, 33 homozygous EP_1-deficient ($EP_1^{-/-}$)and 28 wild-type ($EP_1^{+/+}$) mice were given i.p. injections of AOM (10 mg/kg body wt) once a week for 6 weeks. All mice were provided with food and tap water *ad libitum*, weighed weekly and killed with ether at 56 weeks of age. Complete autopsies were performed and, after laparotomy, the entire stomach and intestines were resected and opened longitudinally and the contents were flushed with normal saline. Using a dissection microscope, large intestinal tumors were noted grossly for their location, number and size. The length (*L*), width (*W*) and depth (*D*) of each tumor were measured with calipers and tumor volume was calculated using the formula $V = L \cdot W \cdot D \cdot \pi/6$ (6). Colon tumors and normal tissues were fixed in 10% buffered formalin and embedded in paraffin blocks for histological evaluation. Diagnosis of intestinal tumors using hematoxylin and eosin stained sections was performed according to the classification of Pozharisski (22). Half of the colon tumors sized >~20 mm^3 and normal mucosa from each group were snap frozen with liquid nitrogen for analysis of RT-PCR.

Silver stained nucleolar organizer region protein (AgNOR) count and apoptotic index

Two serial sections (3 μm in thickness) of colon tumors were used for AgNOR staining and *in situ* end-labeling of fragmented DNA using Apo-BrdU-IHC™ (Chemicon International Inc., Temecula, CA). AgNOR staining was carried out according to the method described previously (23). For determination of AgNOR number in cell nuclei, AgNOR was counted on silver stained sections using a microscope at a magnification of ×400. The other sections were stained with Apo-BrdU-IHC according to the manufacturer's instructions. For analysis of apoptosis, only well-defined and darkly stained cells were counted using a microscope. All tumor cells were counted for AgNOR number and apoptotic index in a section of colon tumor. Five tumors in each group provided data for AgNOR count and apoptotic index. The percentage of labeled cells (apoptotic index) was determined by calculating (labeled cell number:total cell number) × 100.

EP receptor and PKN mRNA expression

Using the RT-PCR method, *EP* receptor and *PKN* mRNA expression in colon tumors and normal mucosa was investigated. Total RNA was isolated from colon tumors and normal mucosa using Isogen (Nippon Gene Co. Inc., Tokyo, Japan) according to the manufacturer's instructions. Reverse transcription with random 9mers was used to generate cDNAs from 0.8 μg total RNA extract using reverse transcriptase (AMV Reverse Transcriptase XL) and a Takara RNA LA PCR kit (Takara Biomedical Co. Inc., Tokyo, Japan). The EP_1 receptor (24) and *PKN* (20) primers were made for PCR amplification of the resulting cDNA (Figure 1): forward primer (*a* in Figure 1) for exon I, 5′-CCTGCATCCTGAGCAGCACT-3′ (nt 33–52); reverse primer (*b* in Figure 1) for the middle of exon II, 5′-TGGCGACGAACAACAGGAAG-3′ (nt 293–312); these being considered as reverse and forward primers for *PKN* (nt 4104–4123 and 2882–2901), respectively. The expected PCR products were 280 bp for the EP_1 receptor and 1242 bp for *PKN*. The EP_1 gene is located in the 3′-untranslated region of the *PKN* gene. To investigate the effects of the EP_1 receptor knockout strategy on *PKN* gene expression, we used primers in the *PKN* encoding region as follows: forward primer (*c* in Figure 1), 5′-GAGAAGGCTACTGCGGAGGA-3′ (nt 562–581); reverse primer (*d* in Figure 1); 5′-CGGCCACAAAGTCGAAATC-3′ (nt 824–842). The expected PCR product was 281 bp. The following primers for the other EP receptors and β-actin were used for PCR amplification of the resulting cDNA: EP_2 (402 bp) forward primer, 5′-AGGACTTCGATGGCAGAGGAGAC-3′ (nt 903–925); reverse primer 5′-CAGCCCCTTACACTTCTCCAATG-3′ (nt 1282–1304) (25); EP_3 (438 bp) forward primer, 5′-CCGGGCACGTGGT-GCTTCAT-3′ (nt 657–676); reverse primer, 5′-TAGCAGCAGATAAACC-CAGG-3′ (nt 1075–1094) (26); EP_4 forward primer, 5′-GCCATAGAGAA-GATCAAGTGCCT-3′ (nt 1150–1172); reverse primer, 5′-CCCACTAACCT-CATCCACCAA-3′ (nt 1480–1500) (27); β-actin (203 bp) forward primer, 5′-TCCTCCCTGGAGAAGAGCTA-3′ (nt 763–782); reverse primer, 5′-CCAGACAGCACTGTGTTGGC-3′ (nt 946–965). PCR conditions were 94°C for 120 s and then 30 cycles of 94°C for 30 s, 62–66°C for 60 s and 72°C for 60 s. β-Actin was used as the internal control for normalization of sample amounts. Agarose gels (1.5%) were stained with ethidium bromide. All assays were performed in triplicate.

Statistical analysis

Body weights, tumor incidence, multiplicity, volume and AgNOR count, as well as apoptotic index, were compared between animals with and without EP_1 receptors. Tumor incidence, expressed as the percentage of tumor-bearing animals, was analyzed using Armitage's χ^2 method. Tumor multiplicity, expressed as the mean number of tumors per animal, tumor volume and body weights were analyzed by unpaired Welch's or Student's *t*-test. AgNOR count, expressed mean number of AgNORs per nucleus and apoptotic index, expressed as percentage of cells with positive staining of Apo-BrdU-IH in tumors, were analyzed by unpaired Student's *t*-test. Differences were considered statistically significant at $P < 0.05$.

Results and discussion

Body weight changes for $EP_1^{+/+}$ and $EP_1^{-/-}$ animals during the experiment are shown in Figure 2, values for the latter being significantly greater at 35 and 50 weeks after the first dosing of AOM (38.3 versus 42.0 g, $P < 0.05$ and 39.6 versus 44.6 g, $P < 0.01$, respectively). One $EP_1^{+/+}$ mouse at the age of 30 weeks was found to have three colon tumors diagnosed as adenocarcinomas. Therefore, mice alive on that day were counted as effective animals. At 56 weeks of age all survivors were killed and complete autopsies were performed. $EP_1^{-/-}$ mice without AOM treatment had no tumors in their intestines and lived >1 year as previously described (15). No tumors

Table I. Effects of EP_1 receptor deficiency on AOM-induced colon carcinogenesis

Animals	Incidence (% mice with colon tumors)			Multiplicity (tumors/mouse)			Tumor volume (mm^3)
	Total[a]	Adenomas	Adenocarcinomas	Total[a]	Adenomas	Adenocarcinomas	
$EP_1^{+/+}$	16/28 (57%)	0/28 (0%)	16/28 (57%)	0.79 ± 0.82[b]	0	0.79 ± 0.82[b]	75.6 ± 153[b]
$EP_1^{-/-}$	8/26 (31%)	1/26 (4%)	7/26 (27%)[c]	0.35 ± 0.55[d]	0.04 ± 0.19	0.31 ± 0.54[d]	12.2 ± 11.7[d]

[a]Includes adenomas and adenocarcinomas.
[b]Values represent means ± SD.
[c]Significantly different from $EP_1^{+/+}$ mice by χ^2 test ($P < 0.05$).
[d]Significantly different from $EP_1^{+/+}$ mice by Welch's t-test ($P < 0.05$).

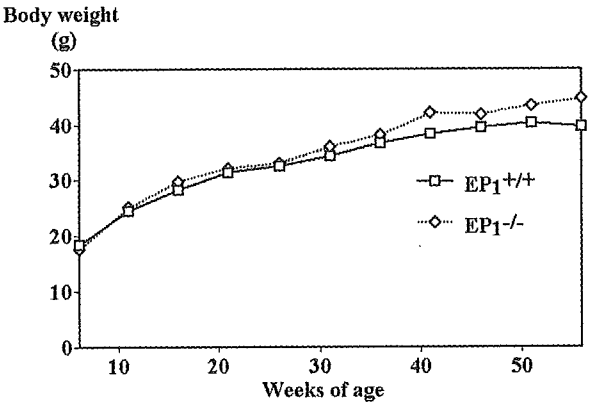

Fig. 2. Body weight changes of $EP_1^{+/+}$ and $EP_1^{-/-}$ mice during the study.

other than colon tumors were observed in AOM-treated mice both with and without EP_1 receptor.

Histopathological examination revealed colon tumors induced by AOM to be adenomas or adenocarcinomas. Table I summarizes the data for effects of EP_1 receptor deficiency on colon tumor development. Colon tumors developed in 8 out of 26 $EP_1^{-/-}$ mice (31%), including 1 mouse with an adenoma and 7 mice with adenocarcinomas. In the $EP_1^{+/+}$ case, 16 out of 28 mice (57%) had adenocarcinomas. In $EP_1^{-/-}$ mice, 0.35 tumors/mouse were found, whereas the value was 0.79 tumors/mouse in $EP_1^{+/+}$ mice ($P < 0.05$). In addition, colon tumor volume was significantly decreased in $EP_1^{-/-}$ mice compared with that in $EP_1^{+/+}$ mice (12.2 versus 75.6 mm^3, $P < 0.05$). Thus, EP_1 receptor deficiency significantly reduced colon cancer development as an end-point. These results strengthen our hypothesis that the EP_1 receptor is involved in colon carcinogenesis and lack of the EP_1 receptor significantly reduces colon cancer incidence and volume.

To elucidate the inhibitory mechanisms, we analyzed cell proliferation and apoptosis in colon tumors of mice with or without the EP_1 receptor. The results are summarized in Table II. Nucleolar organizer regions (NORs) are loops of DNA which contain rRNA genes. They are transcribed by RNA polymerase I and are of vital importance for the ultimate synthesis of proteins (28). AgNORs are acidic proteins associated with the NORs which are selectively stained by a silver colloid technique. A series of studies indicates that the quantity of AgNOR protein is related to the rapidity of cell proliferation and there is evidence of a relationship between AgNOR counts and the prognosis of malignant tumors (29). Mean number of AgNORs per nucleus of tumors in $EP_1^{+/+}$ mice is significantly greater than that of $EP_1^{-/-}$ mice (2.17 versus 1.35, $P < 0.001$). In addition to cell proliferation, we analyzed apoptosis

Table II. Effects of EP_1 receptor deficiency on cell proliferation and apoptosis in colon tumors induced by AOM

Animals	AgNORs count/nucleus	Apoptotic index (%)
$EP_1^{+/+}$	2.17 ± 0.22[a]	0.077 ± 0.067[a]
$EP_1^{-/-}$	1.35 ± 0.11[b]	0.685 ± 0.061[b]

[a]Mean ± SD.
[b]Significantly different from $EP_1^{+/+}$ mice by Student's t-test ($P < 0.001$).

of tumors induced by AOM in both mice. Apoptotic cell count (apoptotic index) in cancers of $EP_1^{-/-}$ mice treated with AOM was significantly higher than that in $EP_1^{+/+}$ mice (0.685 versus 0.077, $P < 0.001$). The mechanisms by which activation of the EP_1 receptor regulates cell proliferation and apoptosis in colon tumors are not known. However, the fact that colon cancers induced by AOM in $EP_1^{-/-}$ mice showed lower cell proliferation rates and higher apoptotic indices than those in $EP_1^{+/+}$ mice suggests that lack of the EP_1 receptor may down-regulate cell proliferation and up-regulate apoptosis, resulting in lower tumor incidence and volume. Further studies to investigate how the EP_1 receptor regulates cell proliferation and apoptosis signaling in colon tumors are required.

To investigate which EP receptors are involved in colon cancer tissues, we analyzed expression of *EP* receptor genes using the RT-PCR method. We first examined the *EP_1* receptor mRNA levels in normal mucosa and cancer tissues in the mice. Representative results on EP receptor expression in normal mucosa and cancer tissues of the colon from $EP_1^{+/+}$ and $EP_1^{-/-}$ mice are shown in Figure 3. Using primers *a* and *b* (Figure 1) we found that the EP_1 receptor was evident in colon cancer, whereas it was not detectable in normal mucosa of $EP_1^{+/+}$ mice (Figure 3, upper panel). As expected, *EP_1* receptor mRNA was not detected either in normal colon mucosa or cancer tissues of $EP_1^{-/-}$ mice. The whole mouse *EP_1* receptor gene is contained within the 3′-untranslated region of a long *PKN* gene transcript. Primers *a* and *b* (Figure 1) were designed to distinguish *EP_1* receptor from *PKN* by product length. Although *PKN* was found to be constitutively expressed in both normal mucosa and cancer of the colon in $EP_1^{+/+}$ mice, interestingly, *PKN* appeared not to be expressed in $EP_1^{-/-}$ mice. These results suggest that the *EP_1* gene knockout strategy may influence the stability of the long form of the *PKN* gene. To clarify the contribution of *PKN* gene instability in *EP_1* knockout mice during colon carcinogenesis, we examined whether the PKN encoding region was influenced in these mice. Using primers *c* and *d* (Figure 1) we found no differences in mRNA levels of the PKN encoding region between normal mucosa and cancer of the colon in both $EP_1^{+/+}$ and $EP_1^{-/-}$ mice (Figure 3, second panel). In addition, expression of